Optimal Drilling

Expanding the Applications of Modal Analysis

Table of Contents

This project is made in collaboration with:

Funding:

INDUSTRIENS FOND

Contributors:

1 Executive Summary

An upgraded version of the TXF software used for tap testing was acquired by DAMRC in 2022. The new software has additional options to enhance process optimisation, including extra cutting modules tailored to tap testing and optimizing more machining processes. The activities in this project focused on acquiring insights and competency in the use of two of these new modules that are of particular interest to the Danish industry. These two modules are Helical Milling and Boring. Helical Milling is a machining strategy used in pocket milling in which the cutting tool follows an orbital tool path as it plunges into the work material, while boring is a commonly used operation to enlarge pre-existing holes.

Initial investigations into the software identified several differences in the settings pertaining to configuring the measurement of tool and workpiece FRFs (Frequency Response Functions) and cutting parameters. Subsequently, it was determined that the Helical Milling software does not produce actionable SLDs (Stability Lobe Diagram) due to glitches in the software, while the Boring module had no such issues. The results obtained with the boring modules were then verified by cutting tests conducted in the DMU 80T machining centre at DAMRC.

From the activities of the project, confirmation was obtained that the boring cutting module is suitable for use in the industry, and standard testing procedures and report formats were established. The project can therefore be considered a success according to the criteria stated in the section 5 were achieved. Utilizing the boring module of TXF in relevant process optimization kickstarts or other projects is therefore highly recommended.

2 Introduction

Initial investigations into the 2022, 64-bit version of TXF demonstrate that the software is equipped with 10 different cutting modules that are each specific to unique machining operations or cutting conditions. These modules cover the following operations:

- Milling
- Face/feed milling
- Plunge milling
- Trochoidal milling
- Thin wall milling
- Small tool milling
- Helical milling
- Boring
- Turning
- Blade Milling

It is imperative that the correct module is used for each test case to ensure that the model used in the optimization process is representative of the involved machining mechanics and that the optimization results are accurate, realistic, and useful for the client. However, R&D engineers at DAMRC have historically only used two of the ten cutting modules available, milling and turning.

This project will look into these new software possibilities directed to different types of milling processes to gain even better results when collecting and analysing data for tap test optimization for machining holes. The idea will be to test two of the unused cutting modules, with the highest expected areas of impact for DAMRCs future services being: (1) Helical Milling, for which interest has been expressed by members of industry and (2) Boring, - more relevant parameter feedback drilling operations. The project will be divided into the following stages:

Phase 1: Investigating the effects of the cutting modules - Helix Milling and boring

Reviewing literature and understanding the differences and changes needed in DAMRCs procedure when performing tap tests into drilling processes (helix milling and boring) processes to obtain more precise analysis than previously done with the cutting module "milling". The phase involves understanding the placement of accelerometers, ways to tap and axis of the stability plots. In-house tests will create the basis before making tests in industry.

Phase 2: Test at case company

After midterm review 1-2 companies will be found for testing the helix milling and boring cutting modules, to see how the gained insights performs when meeting industry needs.

Phase 3: Internal and external knowledge transfer

The knowledge created within the three cutting modules calls for updating the standard operating procedure (SOP) that DAMRC has when performing tap tests in industry. Training of all DAMRC Tap Test personnel in using these modules will be prioritized.

This report is organized as follows:

- Scope of the project along with success criteria, risk analysis, and justifying pre-analysis are presented in sections 3 - 7;
- The findings of a literature study on the mechanics, dynamics, and stability of helical milling and boring processes are presented in section 0;
- The design of experiments evaluating the new helical milling and boring cutting modules and the corresponding results are presented in sections 9 and 10, and discussed in 11;
- Finally, concluding remarks and recommendations are given in section 0.

3 Pre-analysis

An analysis of the capabilities and features of the TXF software is conducted to inform the activities of the project, with a view to investigating the potential value of currently unused cutting modules. The different cutting modules are accessed using the drop-down menu in the *Project* tab in the *Setup* window, as shown in Figure 1. While the project application has emphasized the helical milling and boring cutting modules, a select number of additional modules are also considered considering the discussion on the project scope in Section 6. The major features of these modules are presented in the following subsections.

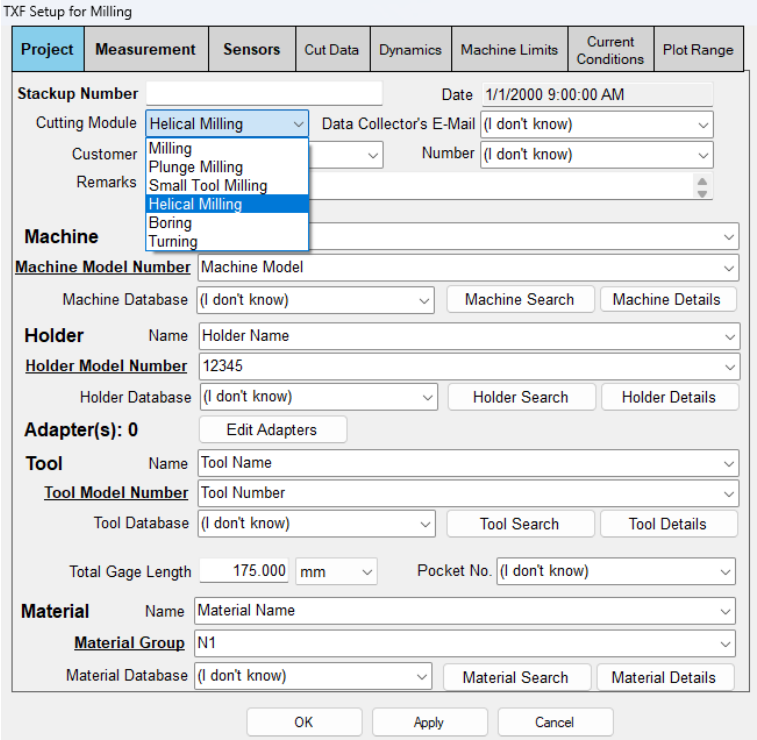

Figure 1 – The project tab of the Setup window in TXF, with the cutting module drop-down menu highlighted.

3.1 Helical Milling

Selecting the "Helical Milling" module in the *Project* tab results in different software settings becoming available in the *Cut Data* tab of the setup window, as shown in Figure 2, while the settings in the other tabs become unchanged. The settings in the *Cut Data* tab for the helical milling module are organized in the same manner as for the standard milling module, in which the settings are divided between "target cutting parameters" and "tool properties," with only the settings for the "target cutting parameters" changing upon switching cutting modules. This reflects the fact that typical milling cutters are used for both machining processes with only the tool path/machining strategy being different.

The new settings reflect the spiral (or helical) path followed by the tool as it plunges deeper into the work material. The tool path is illustrated in Figure 3 and discussed in greater detail in section 8.3 along with the mechanics of helical milling. The settings for the cutting parameters in the cut data tab include the "standard" settings of spindle speed, milling direction, and start and end angle found in the milling module. In addition to this are options to specify stock removal, axial feed per revolution, bore diameter, orbit speed, and milling mode.

Stock Removal, assigned units of millimetres or inches, refers to the linear distance into the work material (Z-direction in Figure 3) the tool travels in the machining cycle, while the Orbit Speed specifies the frequency at which the tool completes one circular orbit in the X-Y plane as shown in Figure 3. The Milling Mode setting specifies whether the tool or the workpiece revolves ("orbits") and in what direction (clockwise or counter-clockwise). Drilling operations can potentially be approximated by setting the bore diameter equal to the tool diameter and setting the orbit speed equal to 0 RPM (as the tool would only rotate about its own axis and would not revolve around the central axis of the bore). After completing the setup process and the enabled FRF measurements, the helical cutting module generates a stability lobe diagram with axial depth of cut on the ordinate axis. Note that the helical milling module is only available in the 2022 (64-bit) version of TXF.

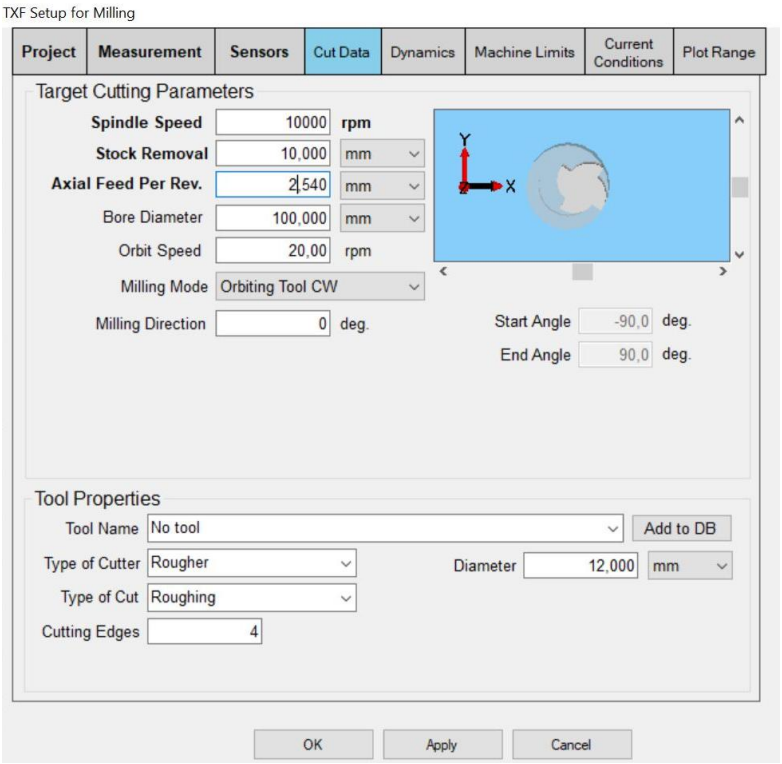

Figure 2 – Cut Data tab when Helical milling module is selected.

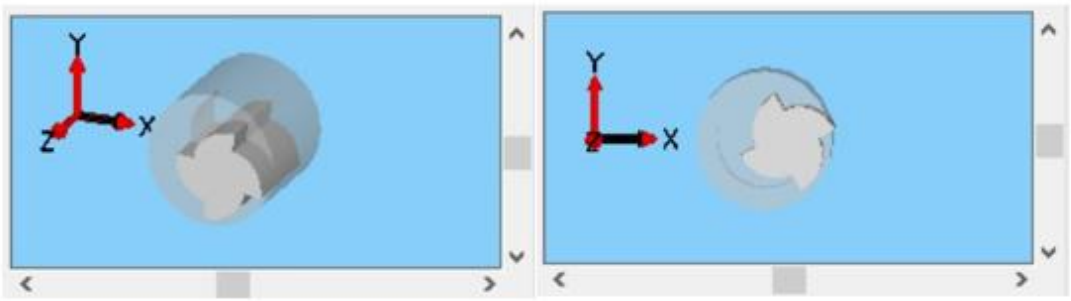

Figure 3 – Illustration of Helical Milling provided by TXF Cut Data tab: isometric view (left) and X-Y view (right). Helical milling involves following a circular toolpath in the X-Y plane while simultaneously feeding into the material (Z-direction), creating a helical or spiral toolpath.

3.2 Boring

Selecting the "Boring" module in the *Project* tab results in changes in the available settings in the *Measurement, Cut Data, and Dynamics* tab of the setup window. The measurement tab is shown in Figure 4. The figure shows that, unlike the corresponding tab for the milling module, options are available for enabling tap test measurements in the z-direction of the tool and workpiece while also removing options for measurements of the cross FRF between the workpiece and tool. Settings in the Dynamics tab are updated to reflect the available measurement locations in the Measurement tab. There is also an option to specify whether the tool or workpiece rotates using the drop-down menu highlighted in the figure.

The Cut Data tab, shown in Figure 5, again organizes the available settings between "cutting parameters" and "tool properties." For the boring module, however, the settings available for "tool properties" is identical to those options available in the Turning module rather than for milling, with the exception that the final bore diameter is specified for boring instead of the part diameter for turning. Besides the typical settings for spindle speed, type of cut, feed rate, and cutting-edge orientation (analogous to milling direction in other cutting modules), there are also options for Boring Mode, stock removal, and maximum feedrate (instead of maximum depth of cut as is the case for milling).

The Boring Mode option has the same effect as the identical setting in the *measurement* tab. Changing the Boring Mode in either tab will update the same option in the other tab. The Stock Removal option allows for the material removed in the boring process to be specified in terms of radial stock removal or diametral stock removal, or else can be calculated by providing the initial and final bore diameters, specified in either millimetres or inches. Drilling operations can potentially be approximated by specifying that the tool (not the workpiece) rotates, setting the final bore diameter equal to the tool diameter, and setting the initial bore

diameter/radial stock removal/diametral stock removal to account for the size of the pilot hole, if any. After completing the setup process and enabling FRF measurements, the module generates a stability lobe diagram having an ordinate axis displaying the radial depth of cut in the 2009 (32-bit) version of TXF; for the 2022 (64-bit) version of TXF the stability lobe diagram has feed rate on the ordinate axis.

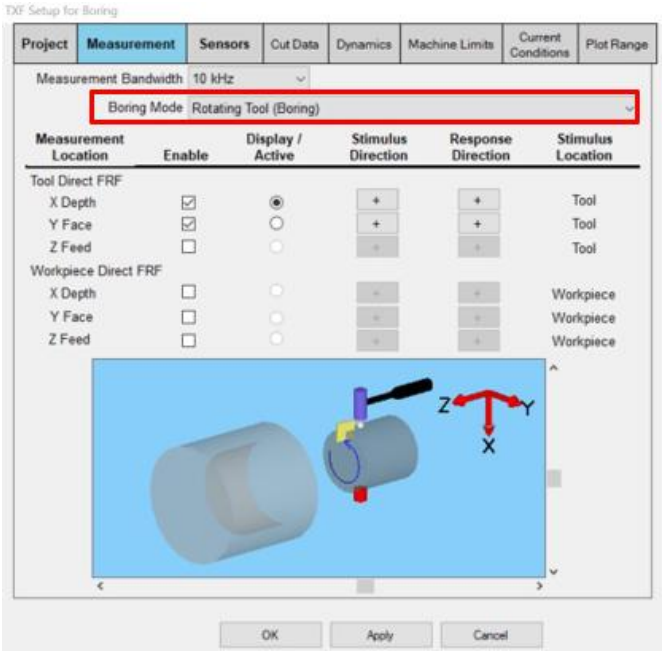

Figure 4 – Measurement tab of the setup window for boring cutting module. The diagram in the figure specifies that the tool is rotating while the workpiece is held stationary. This can be changed by using the highlighted drop-down menu.

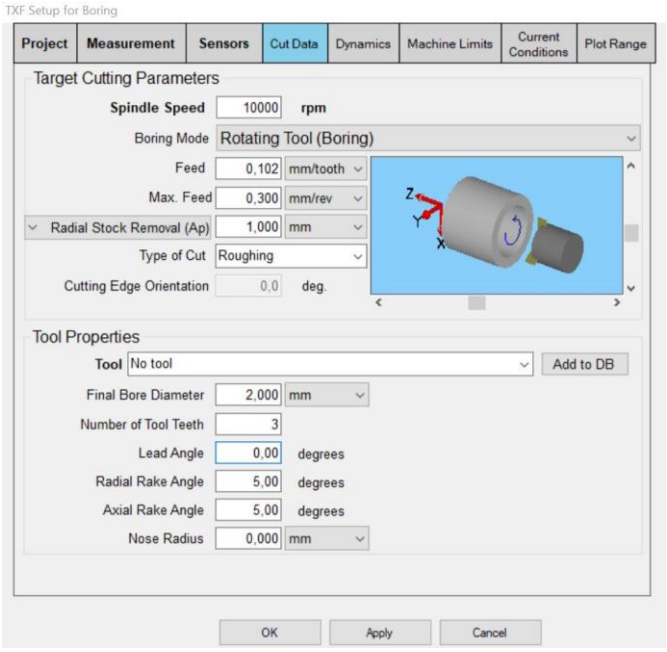

Figure 5 – The cut data tab of the setup window for boring module.

3.3 Plunge Milling

Selecting the Plunge Milling module results in changes in the *Measurement, Cut Data,* and *Dynamics* tab of the setup window. The measurement tab is shown in Figure 6. The settings available in measurement tab for plunge milling are similar to those for boring, with options available to enable FRF measurements in all three coordinate directions of the tool and workpiece and no option to measure cross FRFs between the tool and workpiece. However, there are alternative "cutting modes" as was the case in the boring module. The settings in the *Dynamics* tab are similarly updated to reflect the possible measurement locations in the *measurement* tab.

The Cut Data tab, shown in Figure 7, again organizes the available settings between "cutting parameters" and "tool properties." For plunge milling, the "tool properties" settings resemble those for milling and helical milling cutting modules, reflecting the type of cutter used in plunge milling. Besides the typical settings for spindle speed, type of cut, cutting edge orientation, and feed rate ('plunge feed'), there are options to specify 'plunge mode,' stepover, and engagement depth of cut. These new settings reflect the machining strategy used in plunge milling, which involves feeding the tool into the workpiece along the axial coordinate direction of the tool (Z-direction), as opposed to a radial direction (X- or Y-direction) as is the case for conventional milling. The operation is illustrated in TXF as shown in Figure 8.

After plunging to a predetermined depth into the working material, the tool rapid traverses back to its original position and repeats the machining process at some new X- and/or Y-coordinate. The linear distance in the X-Y plane that the tool travels between operations is specified by the stepover option. The plunge mode option toggles whether full or partial immersion of the tool and also whether the conventional, climb, or custom cutting direction is used. The amount of material engaged in machining during a partial immersion cut is determined by the engagement depth of cut setting. These settings are also subject to the constraint that feed per tooth of the tool must be less than or equal to the cutting length of the tool, and the stepover must be equal to or less than the tool diameter. Breaking these constraints causes an error message to be displayed. A warning is also provided if the engagement depth of cut is too large when the plunge mode is not set to full engagement. Drilling operations can potentially be approximated by setting the plunge mode to full engagement and setting the stepover to 0. After completing the setup process and enabling FRF measurements, the module generates a stability lobe diagram having an ordinate axis displaying feed rate in the 2022 (64-bit) version of TXF (the plunge milling module is not available in the 2009 (32-bit version) of the software.

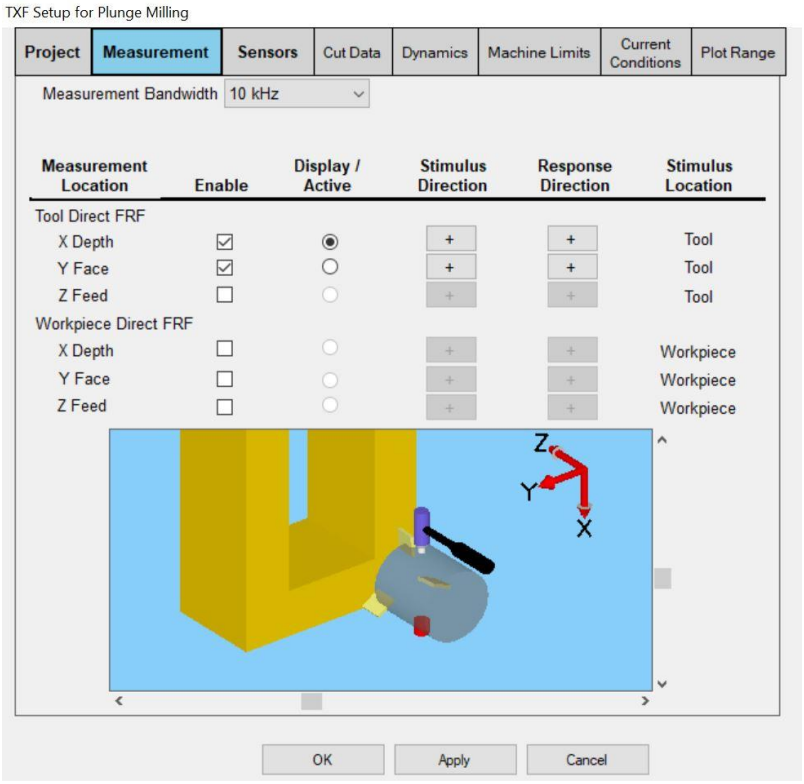

Figure 6 – Measurement tab for plunge milling module.

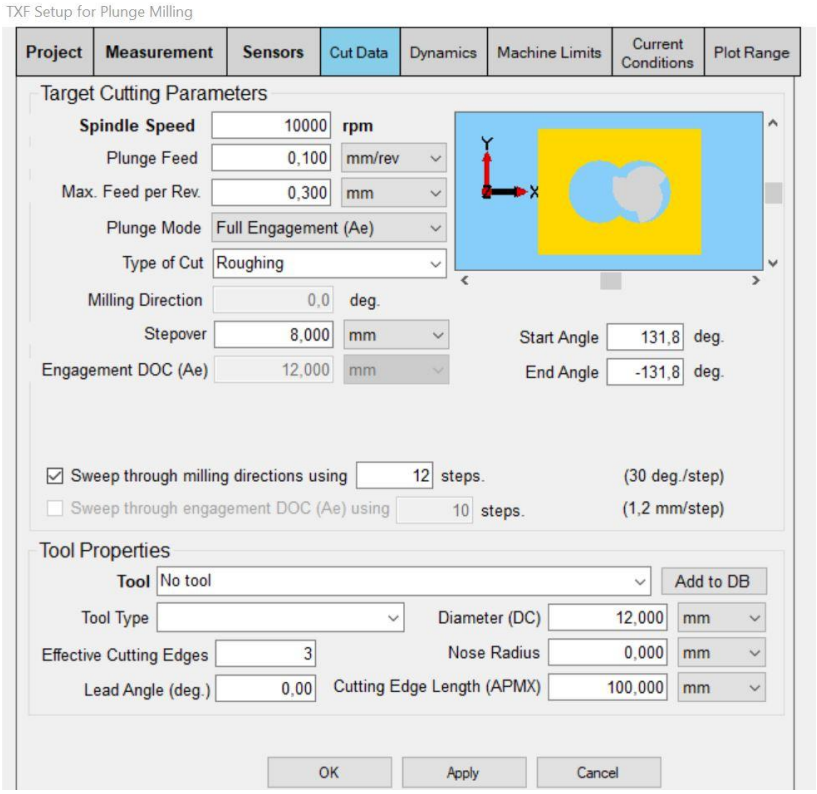

Figure 7 – Cut Data tab for the plunge milling module.

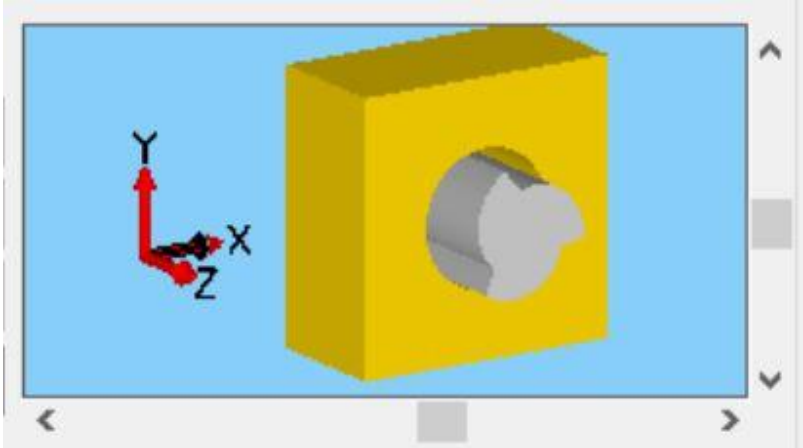

Figure 8 – Illustration in TXF of plunge milling, in which the tool is fed into the work material in the Z-direction. The illustration in the figure above shows full engagement plunge milling with 0 stepover.

4 Hypothesis

There is no formal hypothesis stated in the project application that can be tested. However, the premise of the project is that the boring cutting module in TXF software can be used as an adequate solution to the challenge of optimizing drilling processes.

Furthermore, it is expected that competency and ready-to-use standard operating procedures can be acquired for additional cutting modules within the TXF software, specifically for the Helical Milling and Boring cutting modules.

5 Success Criteria

There is no specific success criteria stated in the project application. However, the goals of the project stated in that document are to achieve competencies and ready-to-use test procedures for the machining processes covered by the helical milling and boring cutting modules, and that these competencies should be also applicable to drilling.

The project can therefore be considered a success when repeatable success in process optimization for these machining processes is achieved both during internal testing and case studies at partner companies. For the results to be repeatable, the test procedures developed during the project should be robust and thorough enough that a non-specialist should be able to completely replicate the test process without resorting to extraordinary measures to achieve the same success under identical test conditions.

6 Project Scope

The scope of the project is defined by the following limitations:

- Existing infrastructure available at DAMRC will be used for the tests: 64- and 32-bit MetalMax TXF software and associated hardware
- Only the two cutting modules listed above (boring and helical milling) will be evaluated during the project.

However, the combination of the above limitation and the stated goal of acquiring competency in optimizing drilling processes is a result of the implicit assumption that the boring module in TXF is the best of all available options for drilling. However, the possibility of a different module being a better option cannot be ruled out, especially when potential discrepancies between the mathematical model used in the boring module and the mechanics of real drilling processes are considered. Therefore, the scope of the project should allow for the investigation of a limited number of additional cutting modules in TXF. Only those modules that can offer a reasonable approximation to drilling should be considered.

7 Risk Analysis

The following risks to the advancement and completion of this project specifically have been identified:

- Tap test results with the new cutting module may yield results that are not fundamentally different from the typically used cutting modules. This can increase the time required for testing as dependencies between various software settings within the software may need to be investigated. This risk is mitigated by reporting such discoveries to the project lead and collaboratively reevaluating how the tests should proceed.
- The cost associated with the tools and other materials required for testing may exceed the funding allocated by the project budget. This risk is mitigated by carefully planning test activities to minimize waste and maximise the useful life of the tool.
- The project can be delayed by unintended damage to the tap test equipment. This risk is mitigated by following standard test procedures when using the tap test equipment and by having contingency plans and appropriate insurance in place to mitigate worst-case scenarios.

8 Literature Study

8.1 Mechanics and Stability Analysis of Drilling and Plunge Milling

Drilling is a machining operation in which a drill, shown in Figure 9, forms a hole by plunging into the workpiece while rotating. The axis of rotation of the drill is typically aligned with the centreline of a pilot hole during drilling which results in a hole having the same diameter as the drill. Unlike end mills which have a similar geometry, the helical flutes only facilitate chip evacuation and does not participate in cutting, which occurs at the chisel edge and cutting lip at the tip of the drill as shown in the figure.

The cutting edge of the drill, having a tapper angle κ_t, is shown in more detail in Figure 10. The cutting forces generated during drilling are distributed along the cutting edge and can be resolved into components in the tangential, radial, and feed directions in tool coordinate system. The overall tangential, radial, and feed cutting forces can be determined from the summation of differential cutting forces along the cutting edge. The cutting forces occurring at each differential element is influenced by the local chip thickness dh and chip height dz, so that the cutting forces are also a function of axial location along the tool, similar to most milling cutters. In drilling, however, the moment arm of the cutting forces changes for each differential element due to the taper angle κ_t. This combined with the plunging nature of drilling process results in significant thrust forces and torsion compared to conventional milling.

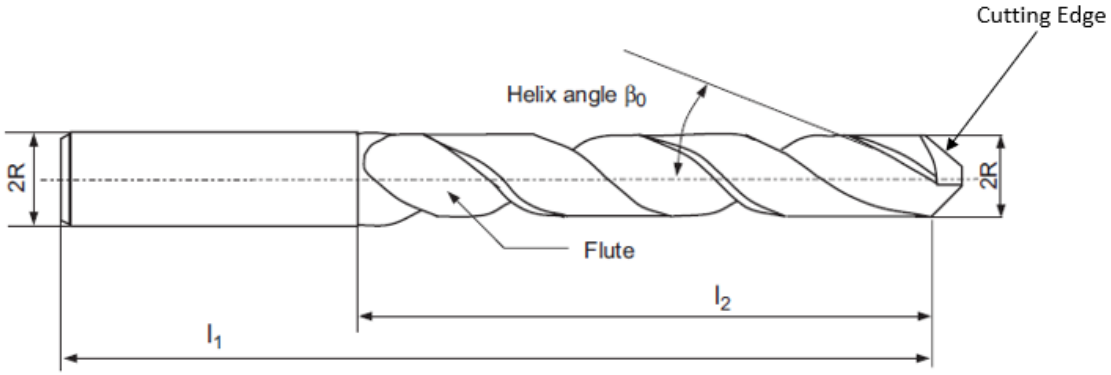

Figure 9 – Twist drill geometry. (Altintas, Manufacturing Automation: Metal Cutting Mechanics, Machine Tool Vibrations, and CNC Design, 2012)

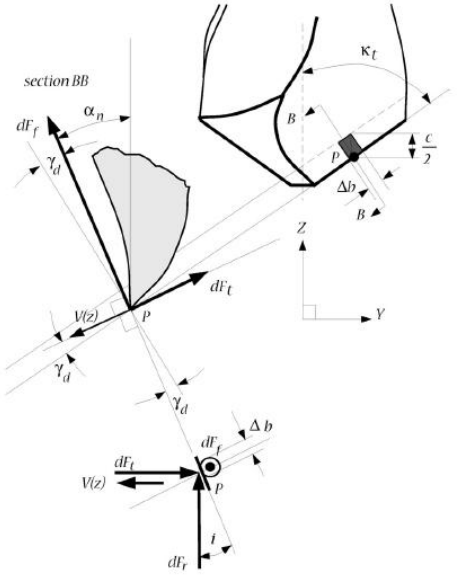

Figure 10 – Detail of cutting edge and cutting forces of twist drill (Altintas, Manufacturing Automation: Metal Cutting Mechanics, Machine Tool Vibrations, and CNC Design, 2012)

The resulting torsion and thrust forces must be considered when considering the dynamic stability of drilling processes. The resulting equations of motion in the stationary frame are expressed as

$$[M]\{\ddot{q}\} + [C]\{\dot{q}\} + [K]\{q\} = \{F\} \quad \text{Eq 1}$$

where the [M], [C], and [K] are the lumped mass, damping, and stiffness matrices, respectively, and the vector {q} is defined as

$$\{q\} = \begin{Bmatrix} x \\ y \\ z \\ \theta \end{Bmatrix} \quad \text{Eq 2}$$

describe the lateral (x, y), axial (z), and torsional (θ) displacementsFigure 11. The force vector {F} is defined as

$$\{F\} = \begin{Bmatrix} F_x \\ F_y \\ F_z \\ T \end{Bmatrix} \quad \text{Eq 3}$$

which consists of the lateral (x, y) and axial (z) forces as well as torsion. Using the equations of motion and direction-dependent cutting coefficients are combined to relate the regenerative displacements of the drill to the dynamic cutting forces, chatter stability can be predicted by solving for the critical depth of cut in the

frequency domain using a procedure similar to that used for chatter stability in milling. For drilling process, however, it is found that axial and torsional vibrations are coupled, while the lateral vibrations are decoupled from the axial/torsional vibrations (Altintas, Manufacturing Automation: Metal Cutting Mechanics, Machine Tool Vibrations, and CNC Design, 2012). Furthermore, it is also found that the torsional vibrations are influenced by the feedrate of the drill (Altintas, Manufacturing Automation: Metal Cutting Mechanics, Machine Tool Vibrations, and CNC Design, 2012).

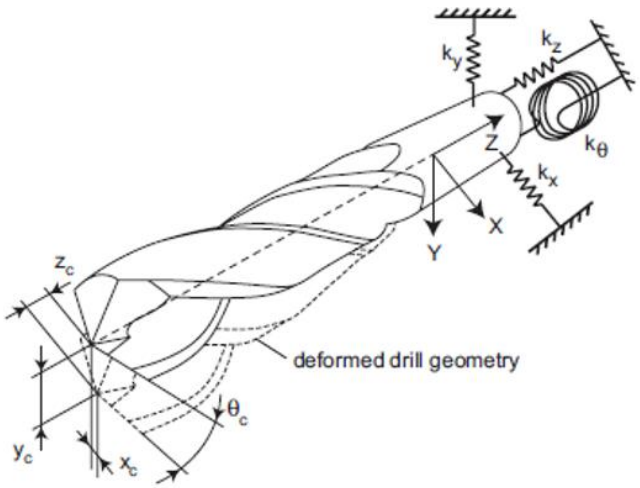

Figure 11 – Deformed drill geometry (Altintas, Manufacturing Automation: Metal Cutting Mechanics, Machine Tool Vibrations, and CNC Design, 2012)

As the drill plunges into the workpiece material, the critical depth of cut solved for in the associated eigenvalue problem refers to the depth of cut in the radial direction. Therefore, the procedure for reducing the depth of cut in drilling to induce a stable cutting process is to increase the diameter of the pilot hole, thereby decreasing the total amount of material removed during machining. An example of a stability lobe diagram for drilling is shown in Figure 12. Similar results are obtained for plunge milling which is illustrated in Figure 13 (Altintas, Chatter Stability of Plunge Milling, 2006).

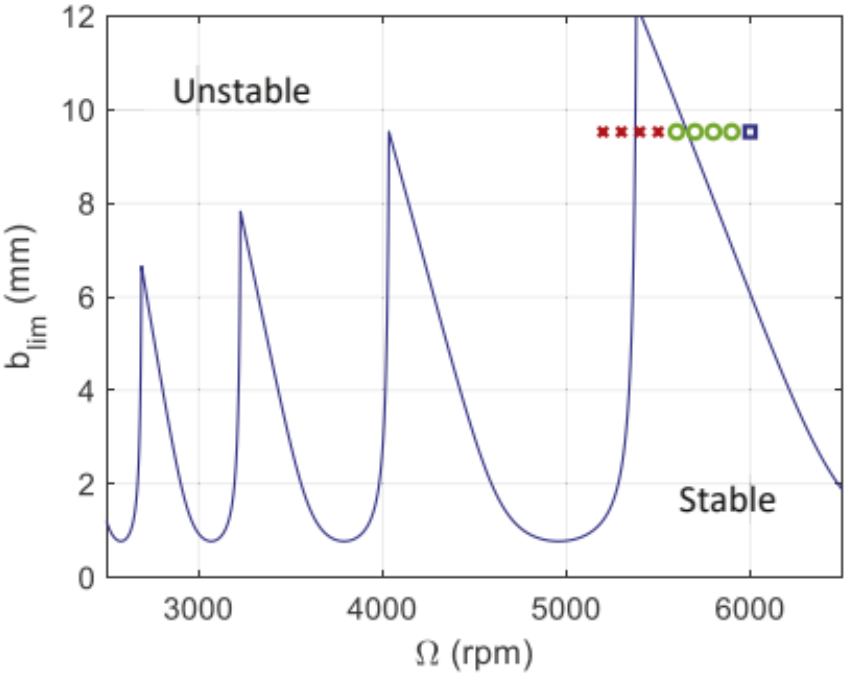

Figure 12 – Stability lobe diagram for drilling (Schmitz, 2020)

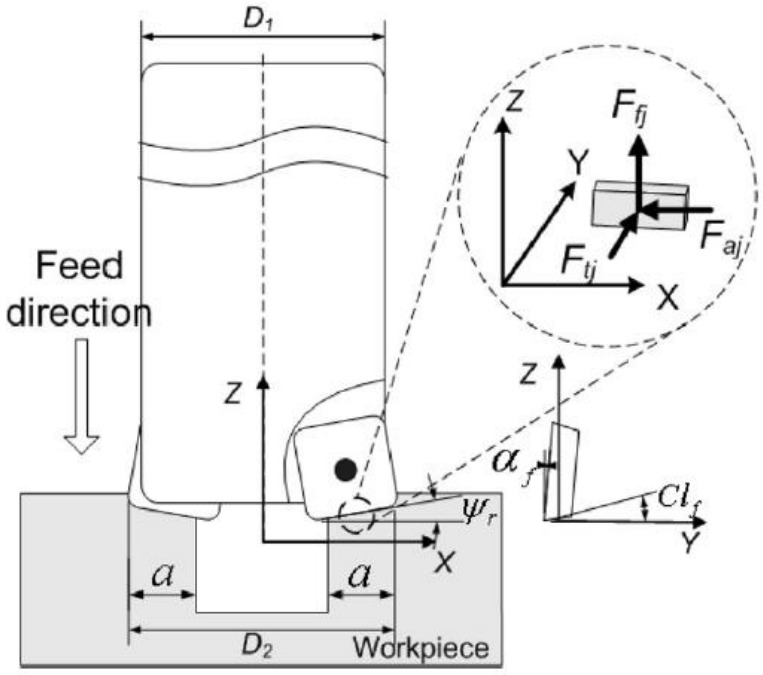

Figure 13 – Geometry and cutting forces of plunge milling. Depth of cut "*a*" influences chatter stability (Altintas, Chatter Stability of Plunge Milling, 2006)

8.2 Mechanics and Stability Analysis of Boring

Boring is a machining operation that typically enlarges an already existing hole, where the tool is fed relative to the workpiece along the axis of the hole. Boring can be achieved by rotating either the tool or the workpiece. Figure 14 illustrates a boring operation where the non-rotating tool is fed along the rotating workpiece. Boring with a non-rotating tool evidently resembles turning, with the caveat that friction and edge forces are much more significant in boring, and that the geometry of the uncut chip area is greatly influenced by the corner radius and feedrate of the tool as well as the radial depth of cut (Altintas, Mechanics of boring process - Part I, 2003). A detailed distribution for representative cutting geometry is presented in Figure 15 and Figure 16 illustrates how the uncut chip geometry varies with feedrate and corner radius.

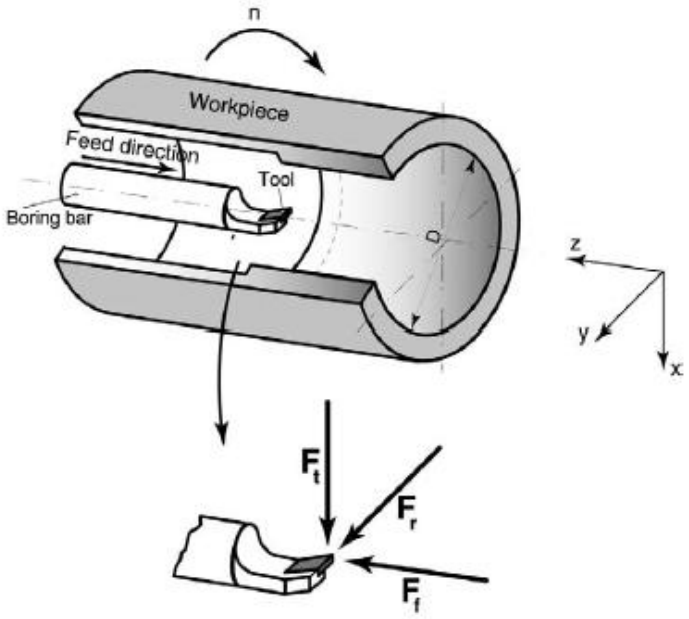

Figure 14 – Boring with rotating workpiece (Altintas, Mechanics of boring process - Part I, 2003)

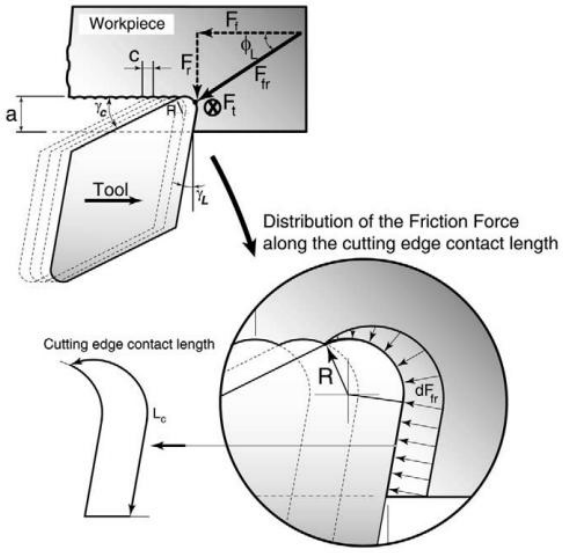

Figure 15 – Distribution of friction force along the contact edge of the boring insert (Altintas, Mechanics of boring process - Part I, 2003)

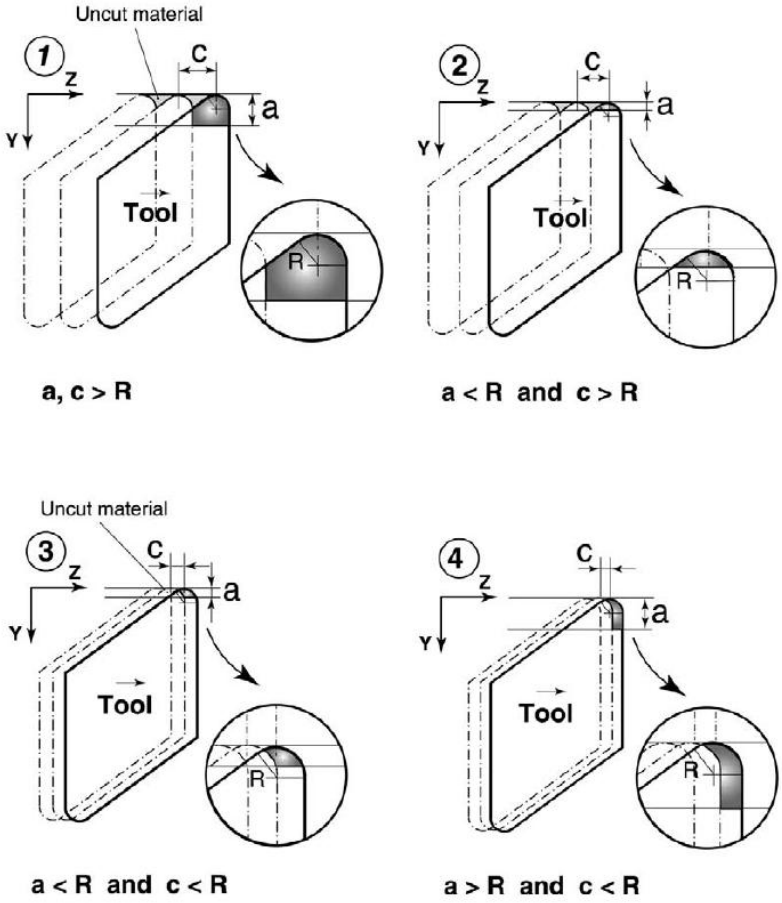

Figure 16 – Variation of chip geometry as a function of radial depth of cut “a”, corner radius “R”, and feed per spindle revolution “c” (Altintas, Mechanics of boring process - Part I, 2003)

Boring operations where the tool is rotating is typically done with boring heads (see Figure 17) having multiple cutting inserts. The cutting mechanics for each individual insert on the boring head can be considered identical to the case of boring with the stationary boring bar discussed above. The overall cutting forces in the boring process with multiple cutting inserts are found from the summation of radial, tangential, and feed cutting forces of all inserts. In general, the cutting conditions depicted in Figure 17 at each insert are assumed to be identical so that the lateral cutting forces are axisymmetric, resulting in a cancellation of the radial and tangential cutting forces in the XY plane. Consequently, the axial cutting and friction forces in the feed direction dominate.

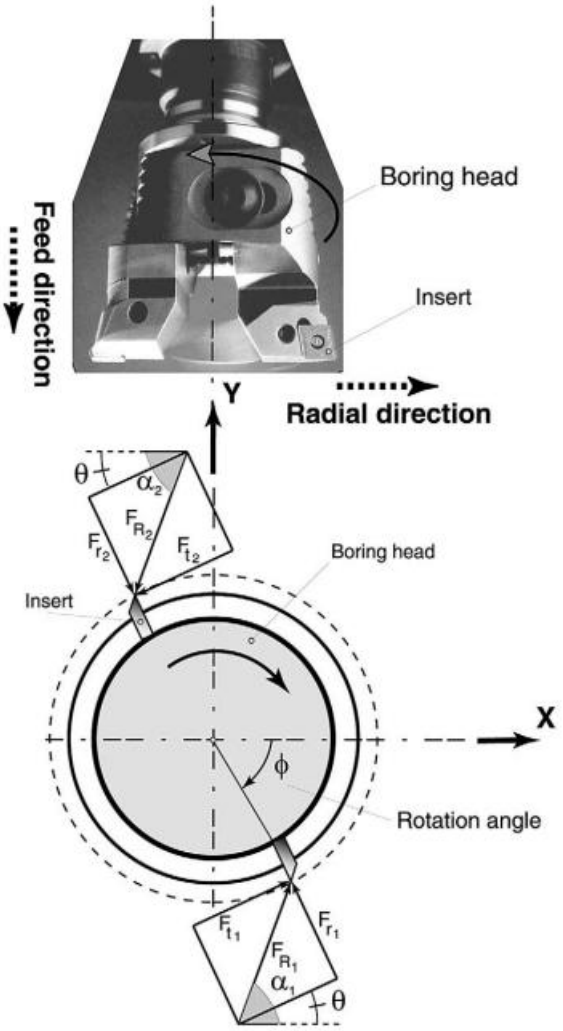

Figure 17 – Illustration of multi-insert boring head and cutting forces (Altintas, Mechanics of boring processes - part II, 2003)

However, the lateral cutting forces may not be axisymmetric in real applications. This can result from improper installation of the cutting inserts, misalignment of the boring head and the hole and runout. Improper installation of the cutting inserts can result in unbalanced lateral and axial cutting forces.

Unbalanced cutting forces can result in tool displacements resulting in time-varying chip loads, leading to regenerative chatter. The issue of process stability is further compounded by the fact that the machined surface left by one cutting insert influences the chip load of the subsequent insert, as is the case in milling. Figure 18 illustrates the difference between an ideal boring process and one in which the radial depth of cut is time-varying. Stability lobe diagrams predicting chatter vibrations can be produced by again deriving expressions for the dynamic cutting forces and solving the corresponding eigenvalue problem in frequency domain. However, the limiting stable depth of cut in boring is shown also to depend on the nose radius of the insert (Budak, 2007).

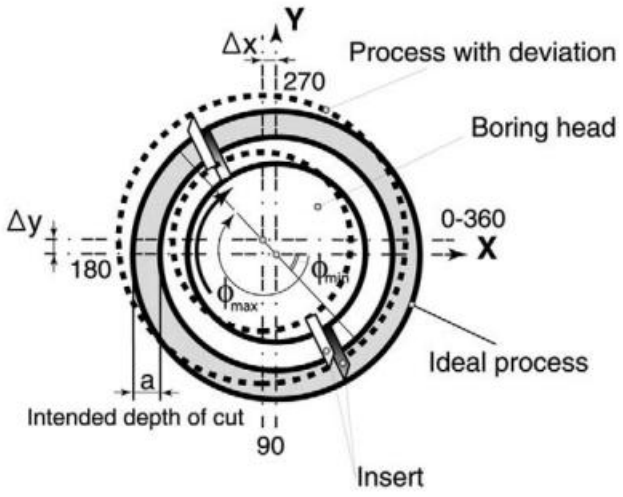

Figure 18 – Variation of radial depth of cut with rotation angle in the case of axis deviation (Altintas, Mechanics of boring processes - part II, 2003)

8.3 Mechanics and Stability Analysis of Helical Milling

Helical milling, also known as orbital drilling or circular ramping, is a machining process in which a hole is formed that is larger than the diameter of the tool. This is achieved by having the tool revolve or orbit around the central axis of the hole while following a helical tool path. The kinematics of helical milling, illustrated in Figure 19, therefore resembles a combination of both peripheral (side) and plunge milling. The interaction between the tool and the workpiece can be divided into separate regions, in which the resulting cutting forces can be described using the cutting mechanics models developed for the simpler machining operations, in which constitute the compound dynamics of helical milling. Analysis of the kinematics of helical milling yields the following equations governing the orbit speed of the tool (n_{rev}) and the axial depth of cut per orbit revolution (or axial feed per revolution, a_p) (Dong, 2014):

$$n_{rev} = \frac{Z n_{rot} f_{zt}}{\pi(D_h - D_t)} \quad \text{Eq 4}$$

$$a_p = \frac{\pi(D_h - D_t) f_{za}}{f_{zt}} \quad \text{Eq 5}$$

where Z is the number of cutting edges of the tool, D_h and D_t are the diameters of the hole and the tool, respectively, and f_{zt} and f_{at} are the lateral and axial feed per tooth of the tool, respectively.

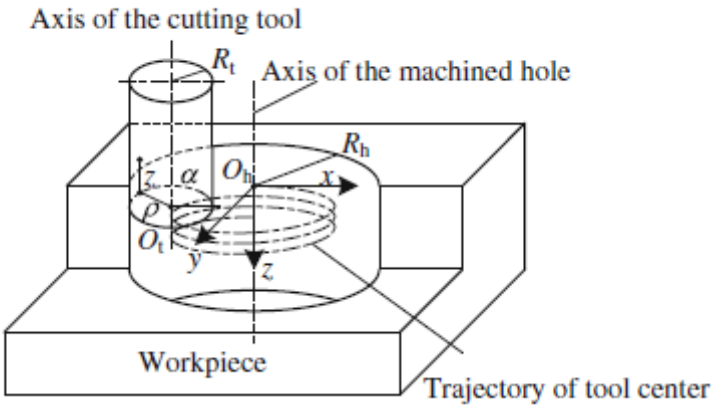

Figure 19 – Kinematics of helical milling (Dong, 2014)

The resulting axial, tangential, and radial cutting forces occurring from peripheral cutting at the side of the tool and from plunge milling at the tip of the tool can be combined to consider overall cutting forces in the helical milling process. The axial rigidity of the tool can be considered comparable to that of conventional milling cutters and the helical machining strategy has the benefit of dramatically decreasing axial cutting forces compared to conventional drilling. As a result, the cutting forces and the corresponding regenerative displacements in axial direction can be neglected in the dynamic cutting model presented in Figure 20 (Dong, 2014). Chatter stability model of helical milling and the corresponding stability lobe diagram can be obtained by extending the zero-order analytic solution in the frequency domain presented by Budak and Altintas, with the critical depth of cut presented in the stability lobe diagram denoting depth of cut per orbit revolution (Dong, 2014).

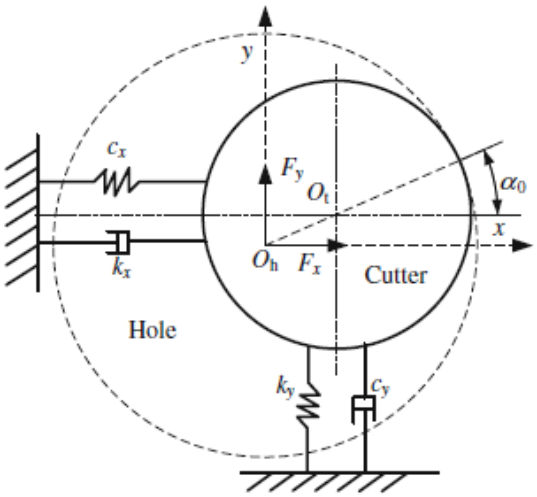

Figure 20 – Dynamic helical milling model (Dong, 2014)

8.4 FRF Measurement Techniques for Machining Holes

In section 8.1 it was noted that regenerative chatter in drilling and plunge milling results in coupled torsional/axial vibrations as well as lateral vibrations, and that the axial/torsional and lateral vibrations are uncoupled. Consequently, conventional techniques for impact modal testing (tap testing) typically utilized at DAMRC for lateral vibrations do not adequately capture torsional/axial vibration modes in the resulting FRFs or SLDs. This is reflected in the fact that selecting both the plunge milling and boring cutting modules in TXF software enables the option to measure the axial (z-axis) FRF of both the tool and workpiece.

Various researchers have investigated measuring the axial, torsional, and axial/torsional FRFs and evaluating the resulting SLDs. Altintas and Ko (Altintas, Chatter Stability of Plunge Milling, 2006) used a miniature hammer and accelerometer to measure the axial, torsional, and axial/torsional FRFs of a plunge mill and validated the resulting SLD with cutting experiments, while Schmitz et. al. (Schmitz, 2020) used a miniature hammer and accelerometer to measure the same FRFs of a twist drill and to quantify the uncertainty of the resulting SLD. The techniques of measuring the axial and torsional vibrations using a miniature hammer are illustrated in Figure 21 and Figure 22. Wei-Hong Zhang et. al. (Zhang, 2019) considered the dynamics of a hole-tapping tool, opting to use an adapter (see Figure 23) made from ultraviolet photo-curable resin. They also modified their stability analysis to account for the added inertia of the adapter and then compared the SLDs resulting from lateral, axial/torsional, and modified axial/torsional FRFs with the results of cutting experiments. A schematic diagram illustrating the FRF measurement strategies using the adapter is shown in Figure 24.

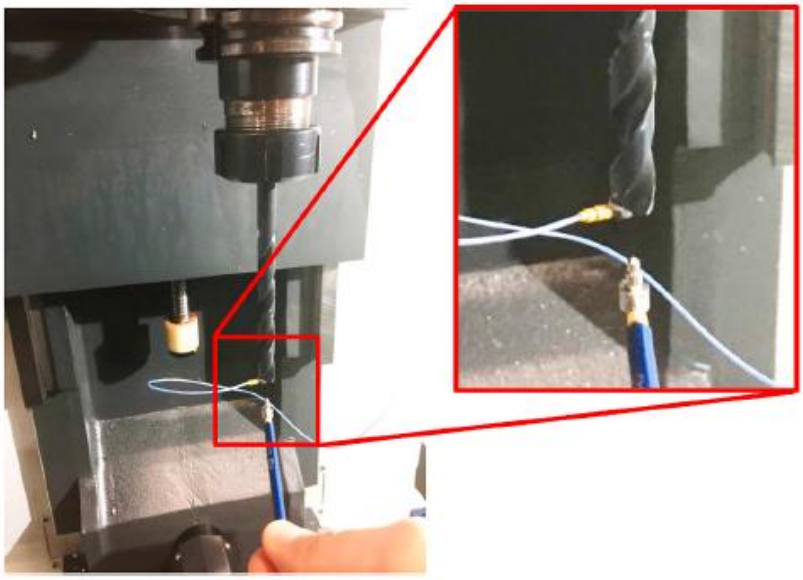

Figure 21 – Axial FRF measurement using a miniature hammer (Schmitz, 2020)

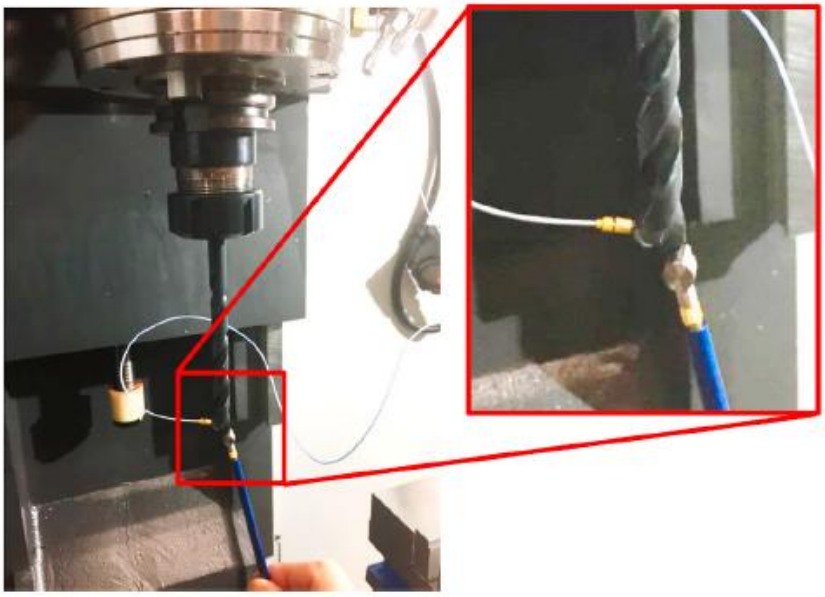

Figure 22 – Torsional FRF measurement using a miniature hammer (Schmitz, 2020)

Figure 23 – Experimental tap test setup using a 3D printed adapter (Zhang, 2019)

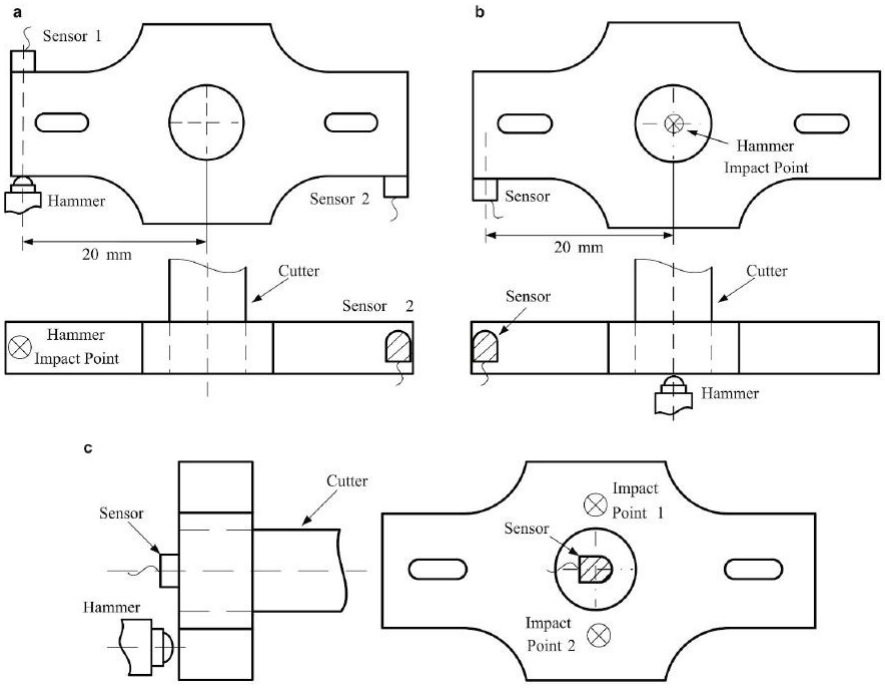

Figure 24 – Schematic diagram for FRF measurement strategies. (a) Torsional FRFs; (b) torsional/axial FRFs; (c) axial FRFs (Zhang, 2019)

8.5 Conclusion of Pre-Analysis and Literature Review

The features, characteristics, and options available in the Helical Milling, Boring, and Plunge Milling cutting modules in the TXF software were investigated and a literature review was conducted to identify the theoretical background informing the dynamic cutting models and stability analysis performed by TXF "under the hood." It was determined that the solution method yielding the SLDs for the new cutting modules in TXF are similar to that used for the stability analysis of milling and turning, but that significant differences exist to account for importance of axial and torsional regenerative deflections and their contributions to process stability.

The literature review also demonstrated that axial/torsional and lateral vibrations are uncoupled in drilling and plunge milling processes and that various researchers have modified their stability models and FRF measurement techniques to capture axial/torsional vibration modes specifically. Comparing the results of the literature review with the pre-analysis of TXF software, it was found that some of the new features in TXF facilitate the measurement of axial/torsional vibrations; however, this is constrained by the locations of the accelerometer and hammer impacts that are enabled by the TXF software. The design of experiments connected to the present project, presented in the next section, will take these findings into account.

9 Experiment Design

9.1 Introduction

Due to the accelerated nature of the current project, planned cutting experiments will be condensed so that only the Helical Milling and Boring cutting modules in TXF will be tested. The test process and required material are described in the following subsections and are subject to change as additional insights are gained from the activities of the project.

9.2 Test Design/Process

The tests of the helical milling and boring cutting modules in TXF will consist of verifying the SLDs produced by the cutting modules with cutting experiments. Therefore, the test process is divided into two phases, (i) measuring the FRFs of the tool(s) to be evaluated and generating the corresponding SLDs and (ii) verifying the accuracy of the resulting SLDs with cutting tests. For conventional drilling processes, the radial depth of cut must be controlled by specifying the diameter of the pilot hole if the same tool is to be used for each test. As a result, verifying the SLD using conventional testing strategies in which depth of cut (or whichever

variable is presented on the ordinate axis of the SLD) is iteratively increased for each cutting trial could dramatically increase the time required to prepare and conduct the experiments. The required cutting tests can become more efficient by avoiding these preparations, which can be achieved by varying spindle speed for each trial while holding depth of cut (or similar variable) constant. The proposed testing strategy is illustrated in Figure 25.

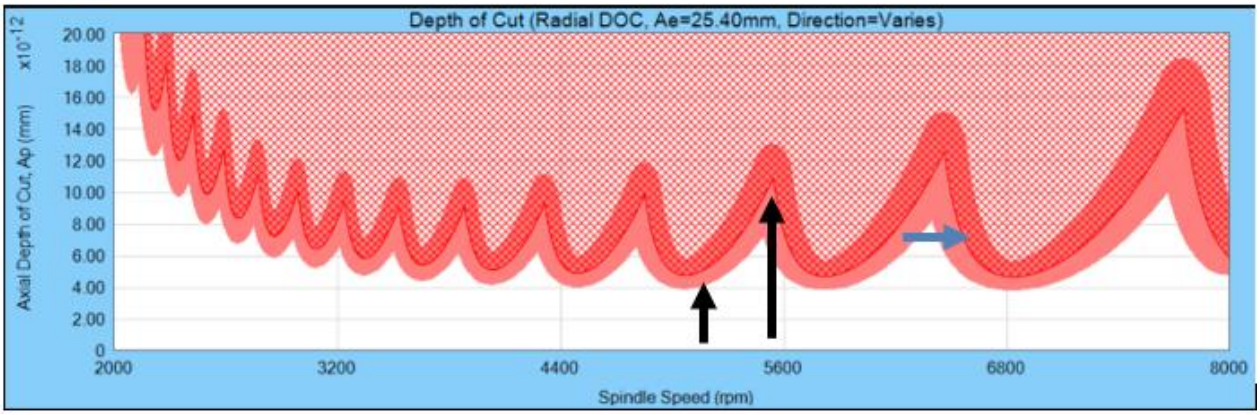

Figure 25 – Conventional (black arrows) and proposed (blue arrow) testing strategies for experimentally verifying SLDs.

The least amount of individual FRF measurements necessary to produce viable SLDs will be conducted in phase (i) to expedite the testing process. Additional tests are carried out to evaluate how implementing different FRF measurement strategies influences the resulting FRFs and SLDs. These different strategies, outlined in section 0, are evaluated using the same testing strategy described above.

9.3 Test Equipment

The tests necessary to derive insights into the optimal use of TXF for machining holes consist of measuring the required FRFs of pre-selected cutting tools and verifying the resulting SLD with cutting tests. Therefore, the items listed in Table 1 are required for testing to be successful.

Description	**Qty.**
64-bit MetalMax Laptop running TXF	1
MetalMax equipment and peripherals necessary for tap testing	1
Plunge milling tool min Ø10 mm	1
Alternate tool for helical milling min. Ø10 mm	1
Other items to be added to the table as required	1

Table 1 – Bill of materials for cutting tests.

In addition, the required cutting tests must obviously be performed in one of the CNC machining centers available at DAMRC. Therefore, a suitable CNC machine, CNC operator, and G-code necessary to implement the prescribed cutting parameters are also required.

9.4 Test Material

The project application indicates that insights gained from conducting boring tests in cast iron are of particular interest to Danish industry. Therefore, cutting tests for both the helical milling and boring cutting modules will be conducted using cast iron stock material available in DAMRC inventories. If cast iron stock cannot be inexpensively sourced, a different workpiece material will be substituted.

9.5 Test Procedure

The overall test of the cutting modules will consist of the following steps:

1. Using the MetalMax equipment to measure the required FRFs of the tool(s).
2. Performing any necessary modal analysis within TXF software to generate the SLD.
3. Generate SLDs, one each for helical milling and boring software modules.
4. In each SLD identify one optimal and one suboptimal spindle speed.
5. For each spindle speed within each SLD, perform successive cutting tests while gradually increasing the variable indicated on the ordinate axis of the SLD. All other cutting parameters are held constant.
6. For each iteration in step 5, record whether the resulting process induced chatter. Compare observed results with SLD-derived predications.

10 Test Results

10.1 Introduction

After conducting a pre-analysis of the new software features in the TXF software and reviewing the available scientific literature concerning boring and helical milling operations, the boring and helical milling cutting modules were internally tested. These tests consisted of performing modal testing (tap testing) of a suitable tool available at DAMRC and placed in the DMU 80T CNC machining center. Tap tests measuring lateral vibration modes were performed with the usual procedures for other tool types as prescribed by the TXF

software. G-code for boring with rotating tool and helical milling operations were prepared for subsequent cutting tests, which were planned according to the testing strategy illustrated in Figure 25.

However, tap testing while using the helical milling cutting module yielded an SLD having no useable results for testing, as shown in Figure 26. Investigations into this issue revealed that the source of the problem appears to be an internal software bug within the TXF software and that the issue is resolved by using a cutting module other than helical milling. This was demonstrated by producing an acceptable SLD using the same FRF data but with a different cutting module and nearly identical settings in the setup window. Consequently, it was determined that further testing of the helical milling module was impossible and that all cutting tests would be focused on the boring module, for which it was possible to generate usable SLDs. The following subsections present in detail the results of the boring cutting tests when the default lateral FRF measurement is used, followed by the results obtained from alternative tap testing techniques.

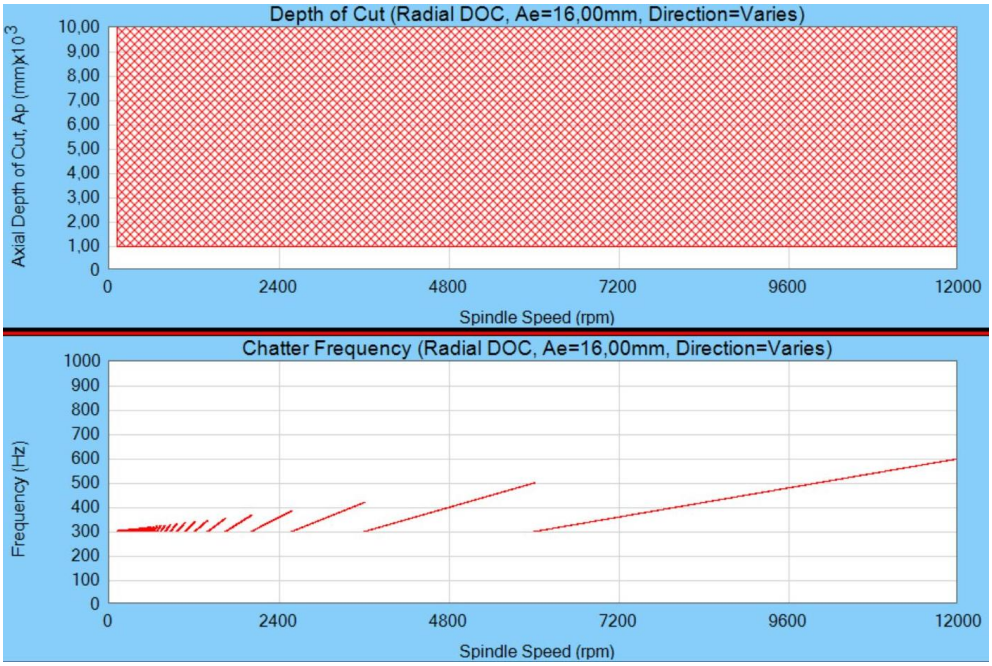

Figure 26 – SLD obtained with helical milling module

10.2 Boring Module Results using "Standard" Tap Test

A square shoulder mill having a diameter of 16mm and 2 cutting inserts was placed in the DMU 80 T CNC machine at DAMRC together with an Erickson Hydroforce tool holder as shown in Figure 27. Tap testing the tool along perpendicular axes to measure lateral vibration modes resulted in the FRF and SLD in Figure 28 and Figure 29, respectively. It was determined that cutting tests should be performed around a spindle speed of 5500 RPM considering the recommended cutting speed from the cutting insert OEM. A test piece of

rectangular mild steel stock material was prepared to facilitate the required cutting tests. Nine pilot holes having a diameter of 10.2 mm were drilled through the entire width of the workpiece. These holes were subsequently bored to a depth of 10mm using the same tool that was tap tested.

Figure 27 – The tool used during the tests of the boring cutting module.

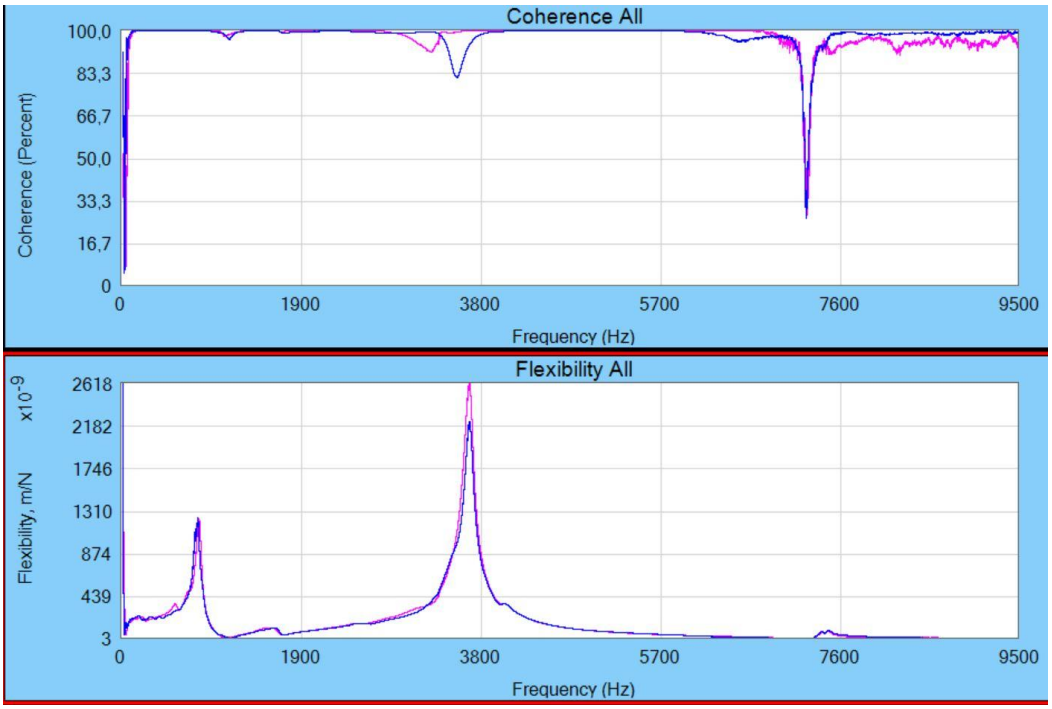

Figure 28 – FRF and coherence obtained from tap testing the tool in Figure 27.

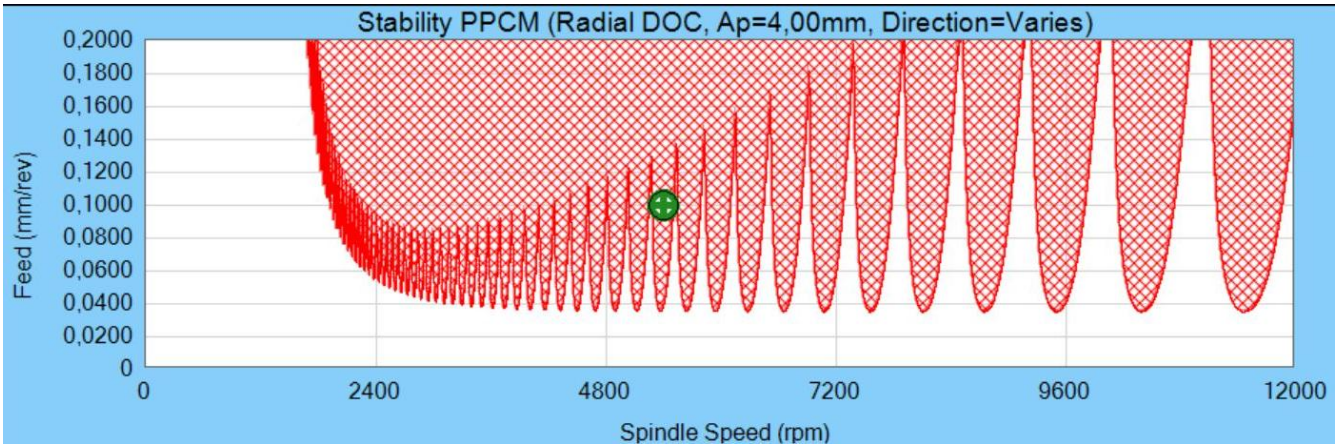

Figure 29 – SLD associated with the tool and data in Figure 27 Figure 28, generated with boring cutting module.

The results of the nine cutting tests are shown in Figure 30, which demonstrates that the results observed during testing are consistent with expected results according to the SLD. The figure shows that the first four cutting tests (including tests with the base cutting parameters labelled as "B") resulted in unstable cutting, as expected. Test "3" also resulted in chatter even though the corresponding parameters are theoretically stable. However, the test parameters fall within the margin of error (which are not shown in the figure for clarity) of the boundary between stable and unstable machining when default uncertainty settings in TXF are used. Adjusting the feedrate at the optimal speed of 5550 RPM further demonstrates stable machining process can be predicted according to the results of the SLD. The presence of chatter was detected from the machining sound emitted during testing as well as the chatter marks left on the workpiece, as shown in Figure 31.

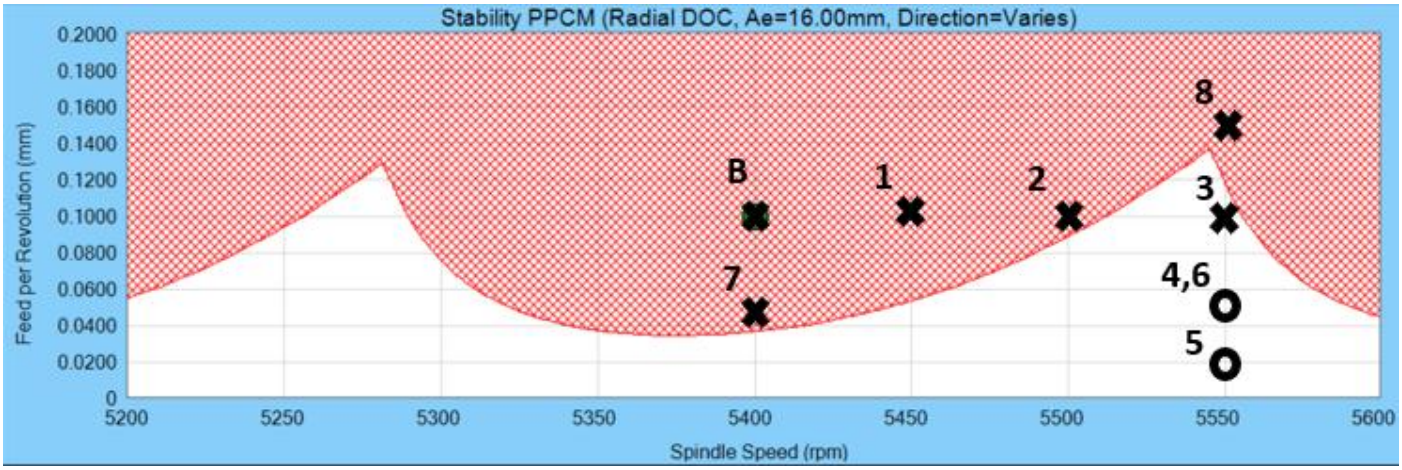

Figure 30 – Detailed view of the SLD in Figure 29, overlaid with the results of cutting tests.

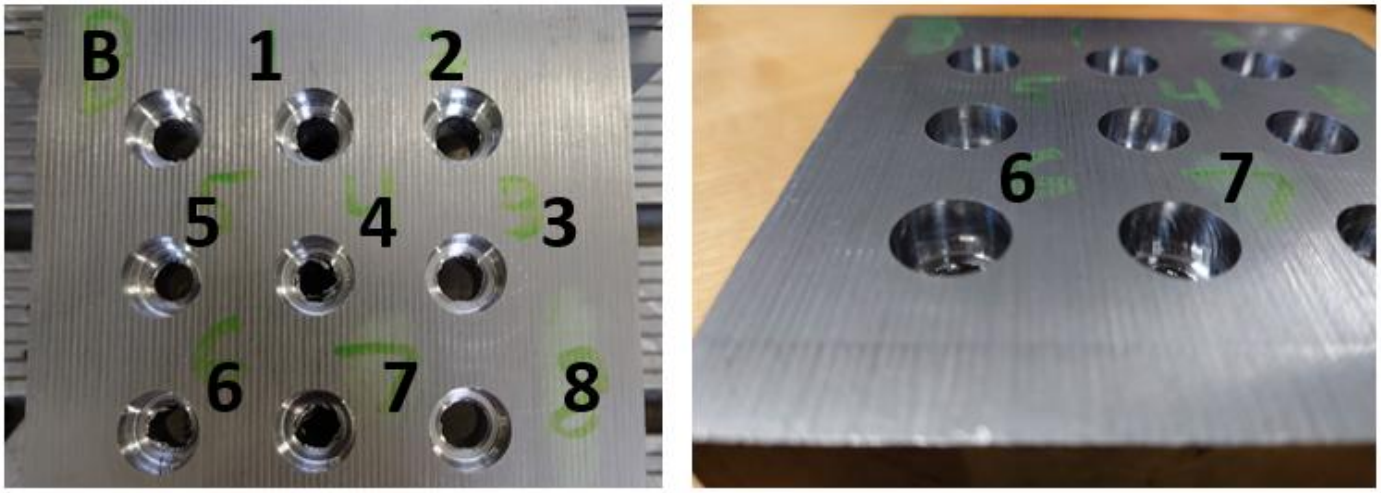

Figure 31 – Bored holes during testing. Left: top view of the test piece; right: detailed view of results 6 and 7, showing the presence of chatter marks when the process is unstable.

10.3 Boring Module Results using "Alternate" Tap Test

Alternative methods of measuring torsional, axial, and torsional-axial FRFs are evaluated following the methods used in (Schmitz, 2020) and (Zhang, 2019). To measure torsional and axial FRFs as described in (Zhang, 2019), the adapter shown in Figure 23 is 3D printed at DAMRC and fitted onto a Ø10mm, 2-flute drill installed in the DMU 80T CNC machining centre as shown in Figure 32. The adapter is used to test the measurement configurations in Figure 24. Additionally, torsional and axial FRFs are measured using the small hammer as described in (Schmitz, 2020) and shown in Figure 21 and Figure 22.

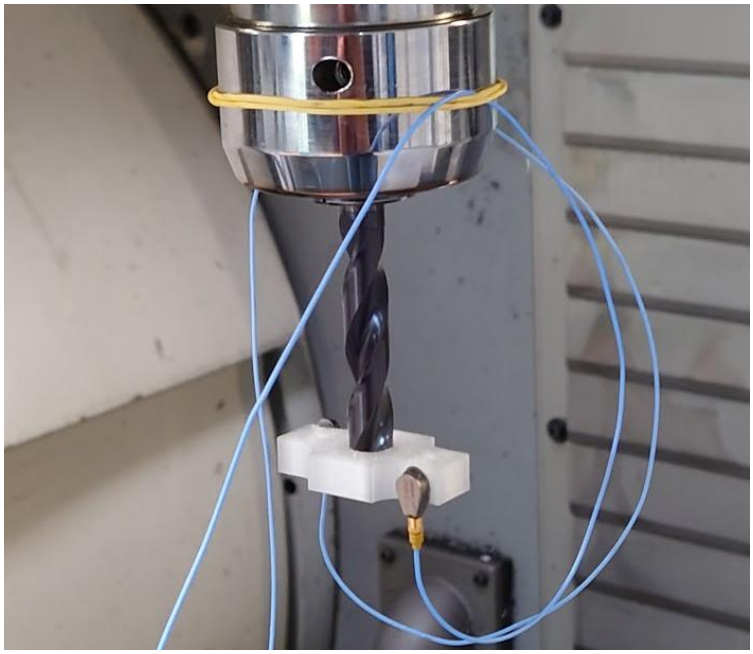

Figure 32 – Test setup for evaluating alternative tap test methods targeting torsional FRFs.

These tests intended to modify these alternative FRFs as prescribed in (Schmitz, 2020) and (Zhang, 2019), if applicable, and import the resulting oriented FRFs into TXF software to obtain the resulting SLDs. However, limitations with the TXF software rendered this option impossible. Therefore, an analysis of the data was performed using Python to generate the modified SLDs. The results obtained with and without the tap test adapter are presented in the following subsections.

10.3.1 Torsional FRF Measurements without Adapter

The resulting torsional FRFs and the corresponding SLDs when using small (PCB 086E80) and medium (Bruel & Kjær type 8206-001) hammer with the small accelerometer (PCB 352O23) in the configuration shown in Figure 22 are presented in Figure 33 - Figure 35. Tap tests in both the x- and y-direction of the tool are obtained to generate the SLDs within TXF using existing standard operating procedures; however, since torsional, not lateral vibration modes are characterized, the measured FRFs are identical for both directions. Therefore, only the FRFs for x-direction are presented alongside the SLDs.

The results indicate that both small and medium hammers are equally suited for capturing torsional vibration modes below 6000 Hz and that the resulting FRFs and corresponding coherence are consistent and of good quality in this frequency range. The SLDs presented in Figure 34 and Figure 35 demonstrate that, while the two SLDs are very similar, slight variations in the FRFs translate to corresponding differences in the SLDs, most notably the major lobes above 7800 RPM. More significant differences exist between the SLDs at lower speeds where process damping effects must be considered.

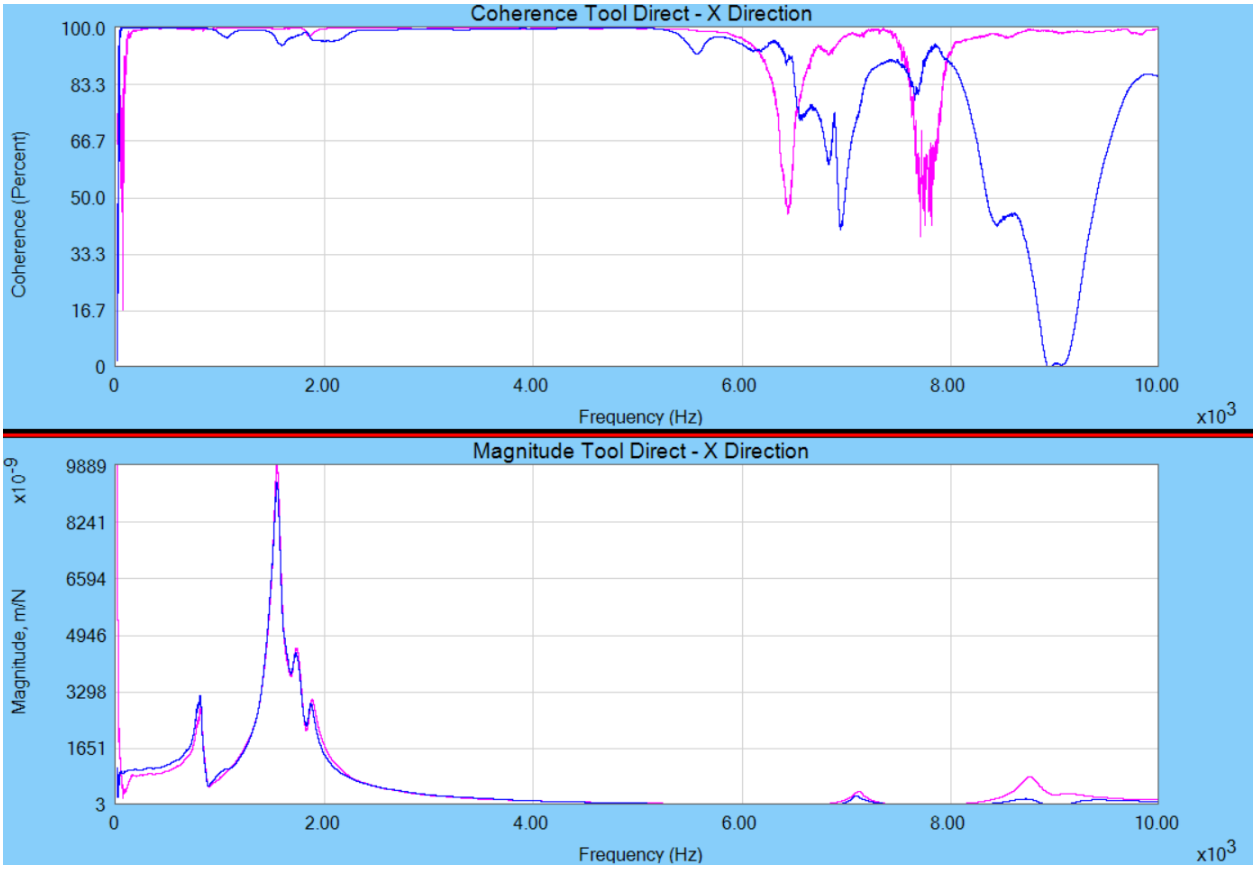

Figure 33 – Torsional FRF and coherence measured without an adapter when the medium (blue) and small (purple) hammers are used.

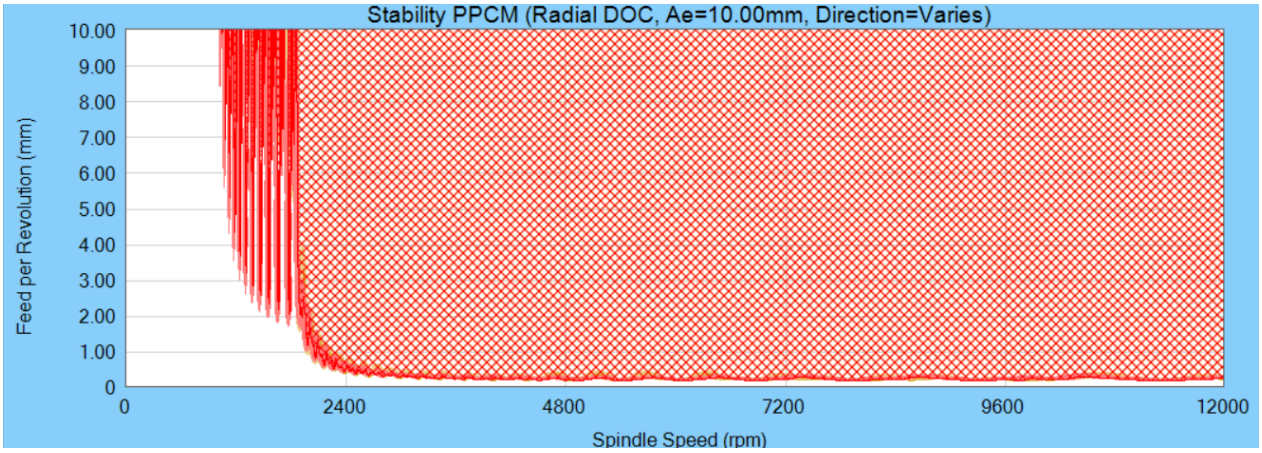

Figure 34 – SLDs obtained for the torsional FRFs shown in Figure 33.

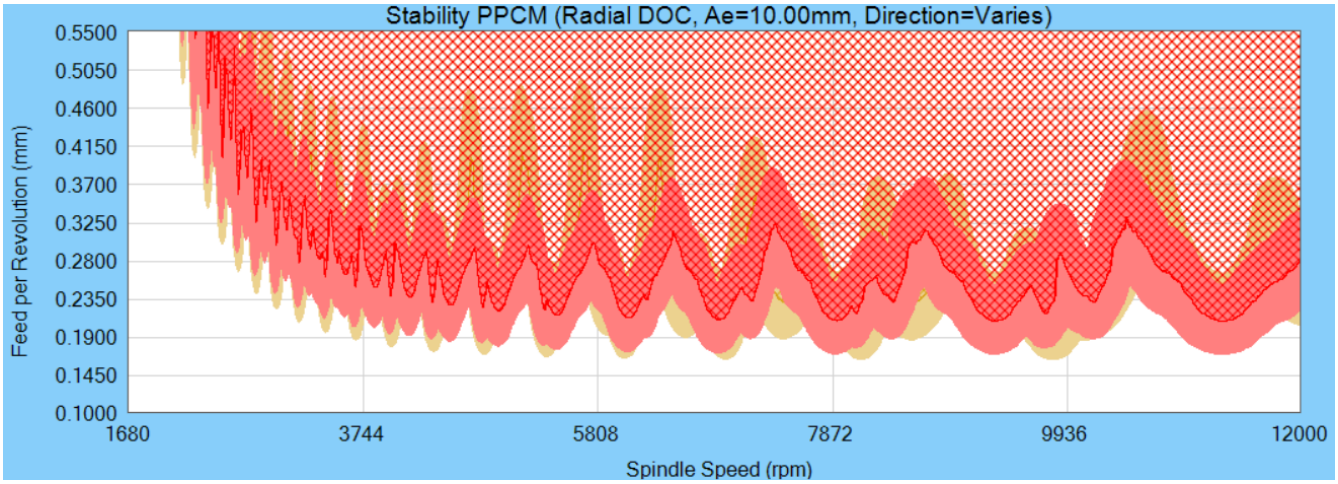

Figure 35 – First detailed view of Figure 34, showing SLDs for medium (red) and small (brown) hammers.

The above results are compared with lateral FRFs and the SLD obtained with medium hammer (Bruel & Kjær type 8206-001) and accelerometer (PCB 352A21), which are presented in Figure 36 and Figure 37 and compared with the torsional SLDs in Figure 38. The results in these figures indicate that SLDs derived from lateral FRFs are characterized by distinctly different optimal spindle speeds and maximal depths of cut, and that these differences are more pronounced at higher spindle speeds (above 8000 RPM in Figure 38). This is consistent with results reported in (Zhang, 2019), which demonstrated that the SLDs resulting from lateral FRF measurements were characterized by a chatter limit occurring at a significantly deeper depth of cut compared to the results obtained for torsional FRFs. However, the results in Figure 38 indicate that the difference in stable axial depth of cut between torsional and lateral FRFs are relatively minor.

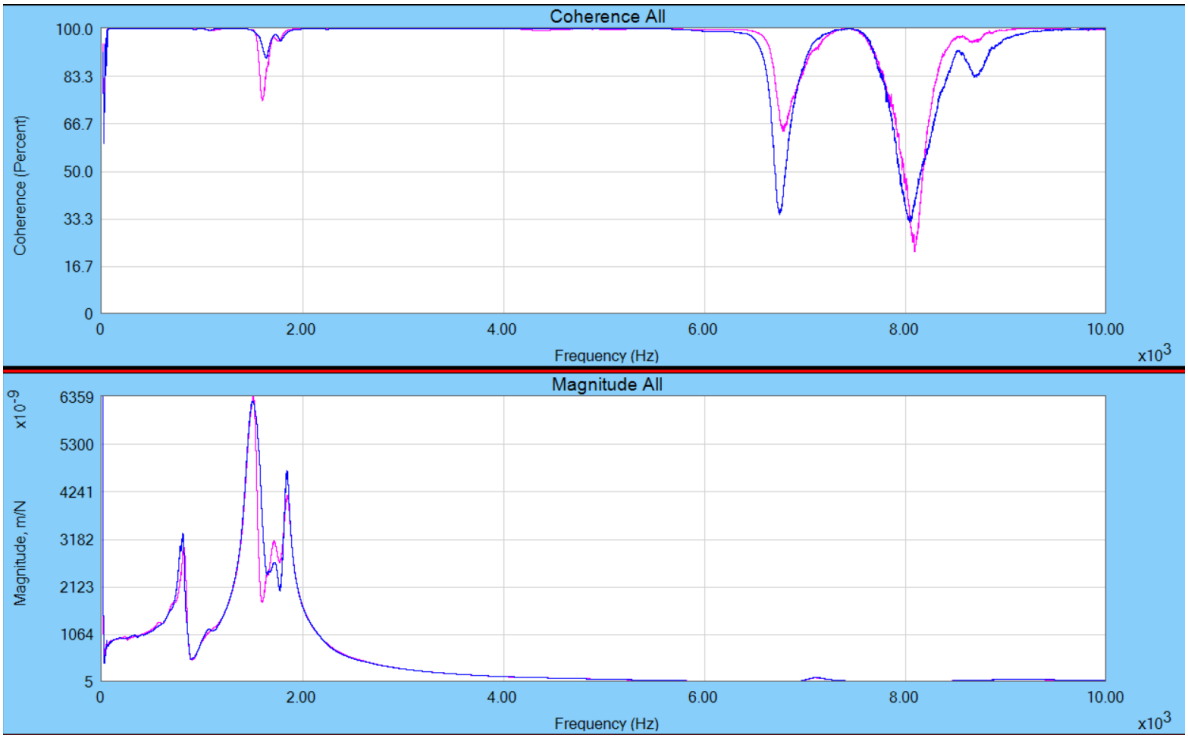

Figure 36 – Lateral FRF in x (blue) and y (purple) directions.

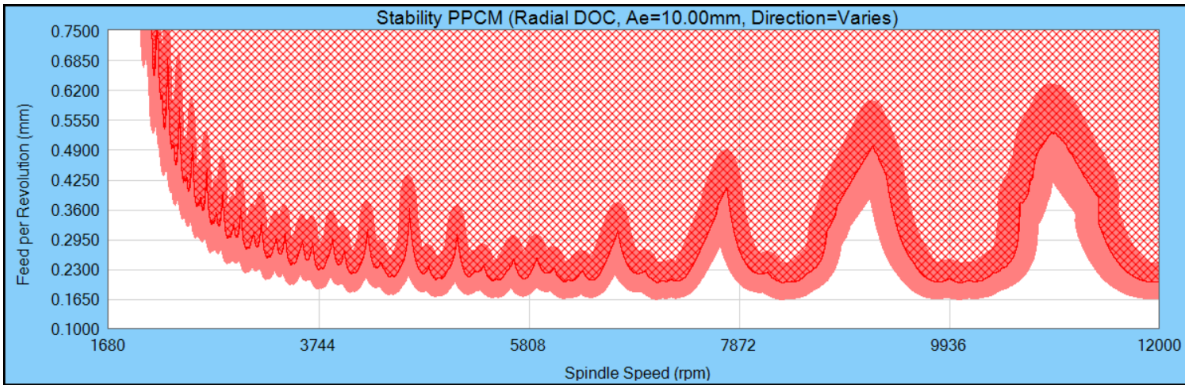

Figure 37 – Detailed view of the SLD produced with the FRF in Figure 37.

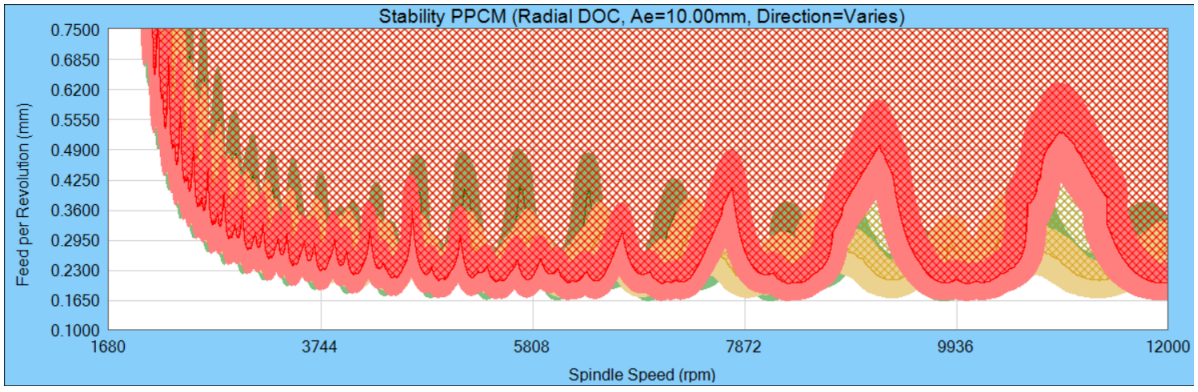

Figure 38 – Lateral (red), torsional with medium hammer (brown), and torsional with small hammer (green) SLDs are presented.

10.3.2 Torsional/Axial FRFs measurements using adapter

Torsional FRFs of the tool are also measured using the 3D printed adapter and testing methods presented in Figure 23 and Figure 24. Since the MetalMax TXF software is designed to analyse one input and one output data channel only, the FRFs are measured using the 'Frequency Response' module of SpinScope 2024. Tap test measurements using a medium hammer (Bruel & Kjær type 8206-001), medium accelerometer (PCB 352A21), and small accelerometer (PCB 352O23) in the measurement configuration shown in Figure 24 (a) and Figure 32 to produce the FRFs presented in Figure 39. The FRFs in the figure are produced using 5 individual hammer impacts where the small accelerometer was used as 'sensor 1' and the medium accelerometer was used as 'sensor 2' with reference to Figure 24 (a). The axial-torsional and axial FRFs are similarly measured using the measurement configurations in Figure 24 (b) and (c), the results of which are shown in Figure 40 and Figure 41, respectively. However, the TXF software is again used since only once accelerometer is necessary in these measurements.

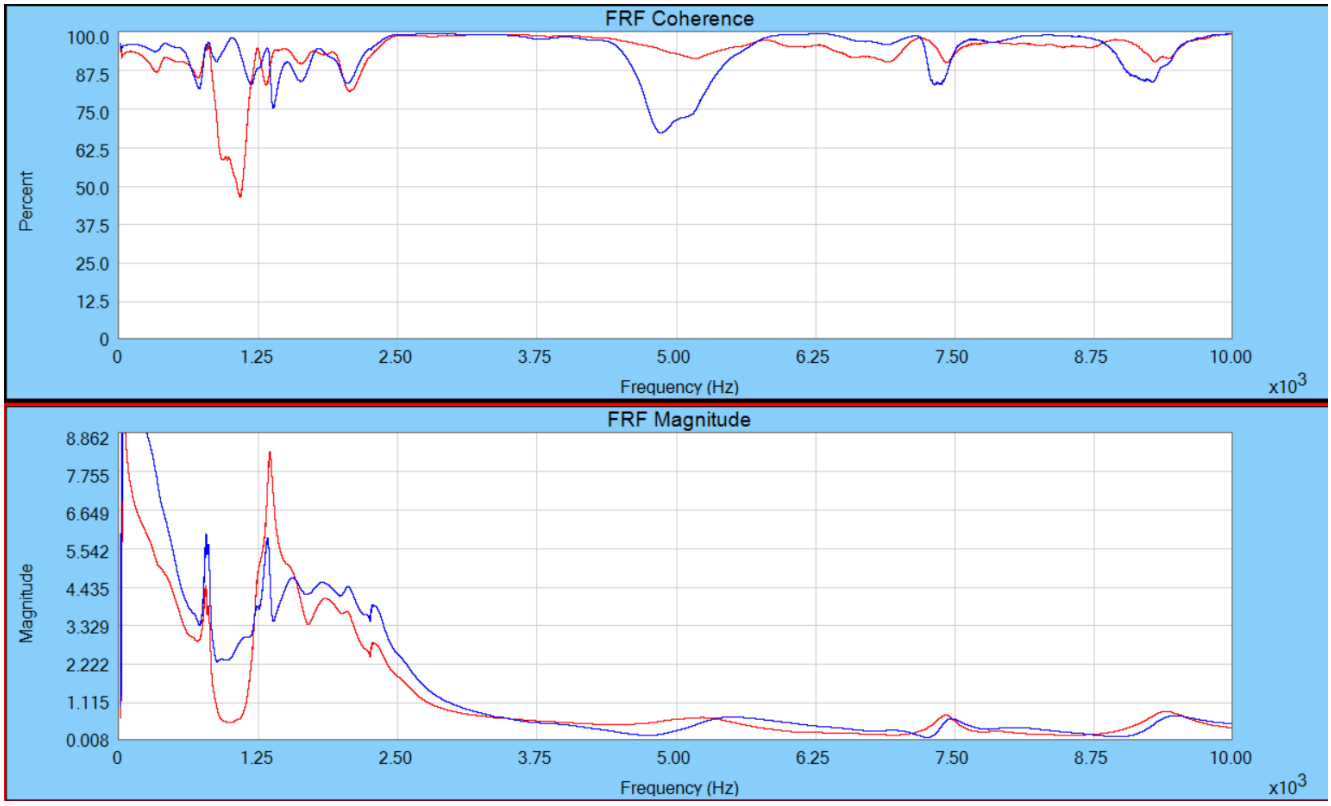

Figure 39 – FRF magnitude and coherence with SpinScope Frequency Response Module and 3D printed adapter. With reference to Figure 24 (a), the FRFs using sensor 1 (blue) and sensor 2 (red) are shown.

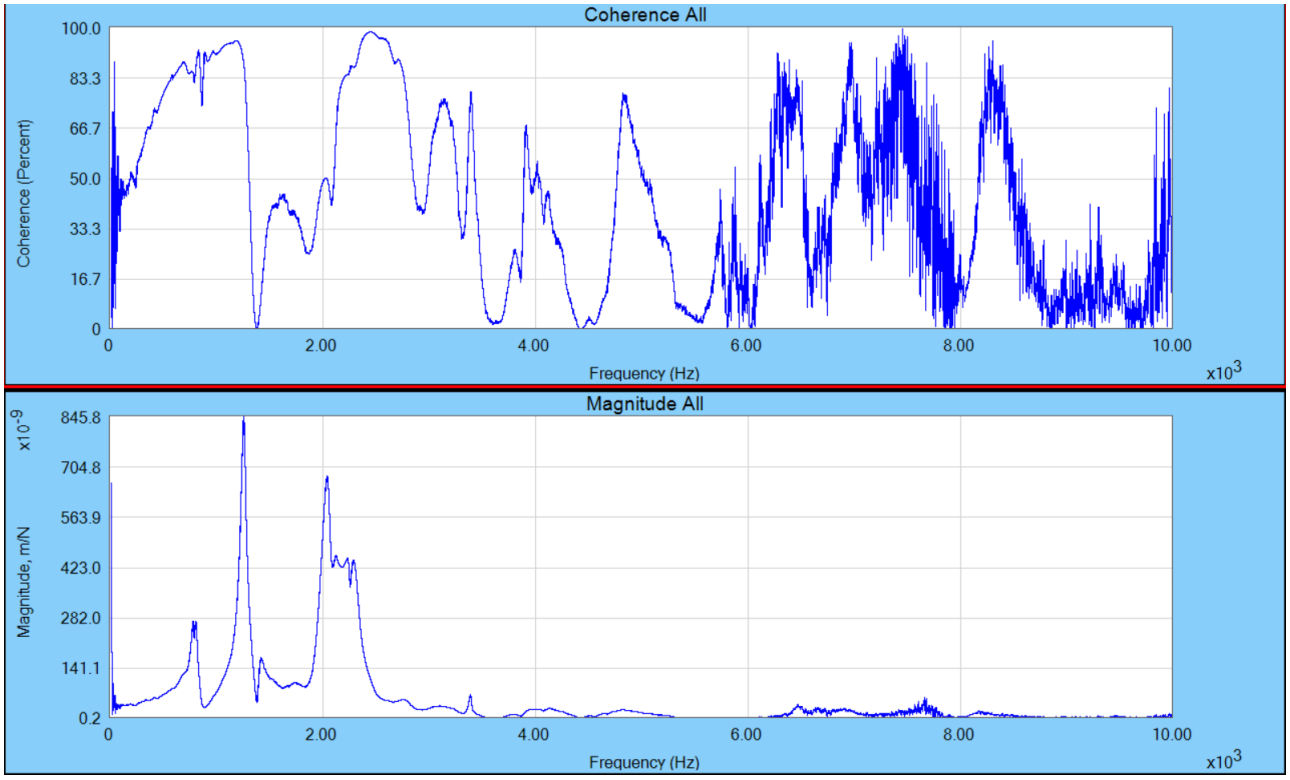

Figure 40 – Axial-torsional FRF and coherence.

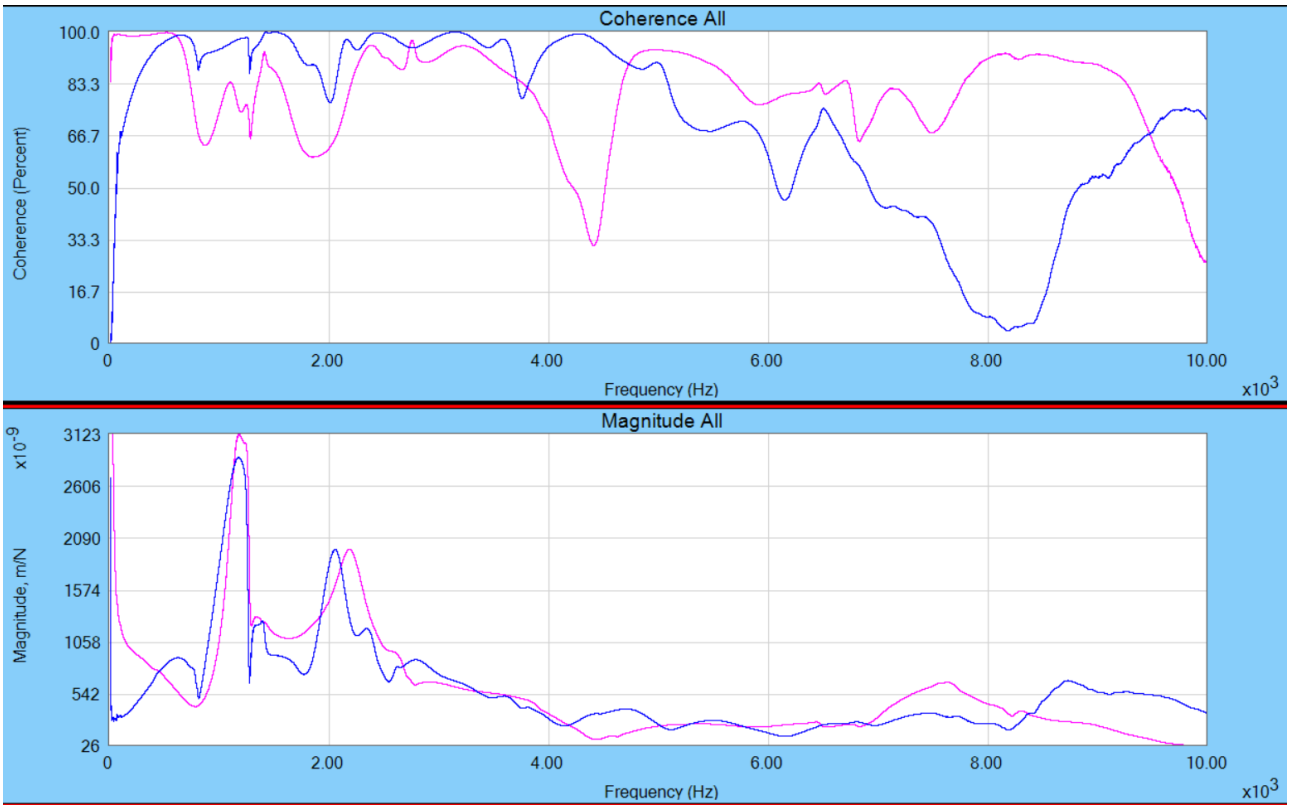

Figure 41 – Axial FRF with accelerometer at locations 1 (blue) and 2 (pink).

The results in Figure 40 and Figure 41 indicate that the magnitude of the axial and axial-torsional FRFs are significantly less than that of the torsional FRF. However, the FRFs shown above are the "raw" measurements and need to be modified to consider the mass and stiffness of the adapter, which is done following the methods outlined in (Zhang, 2019), resulting in the FRF and SLD presented below.

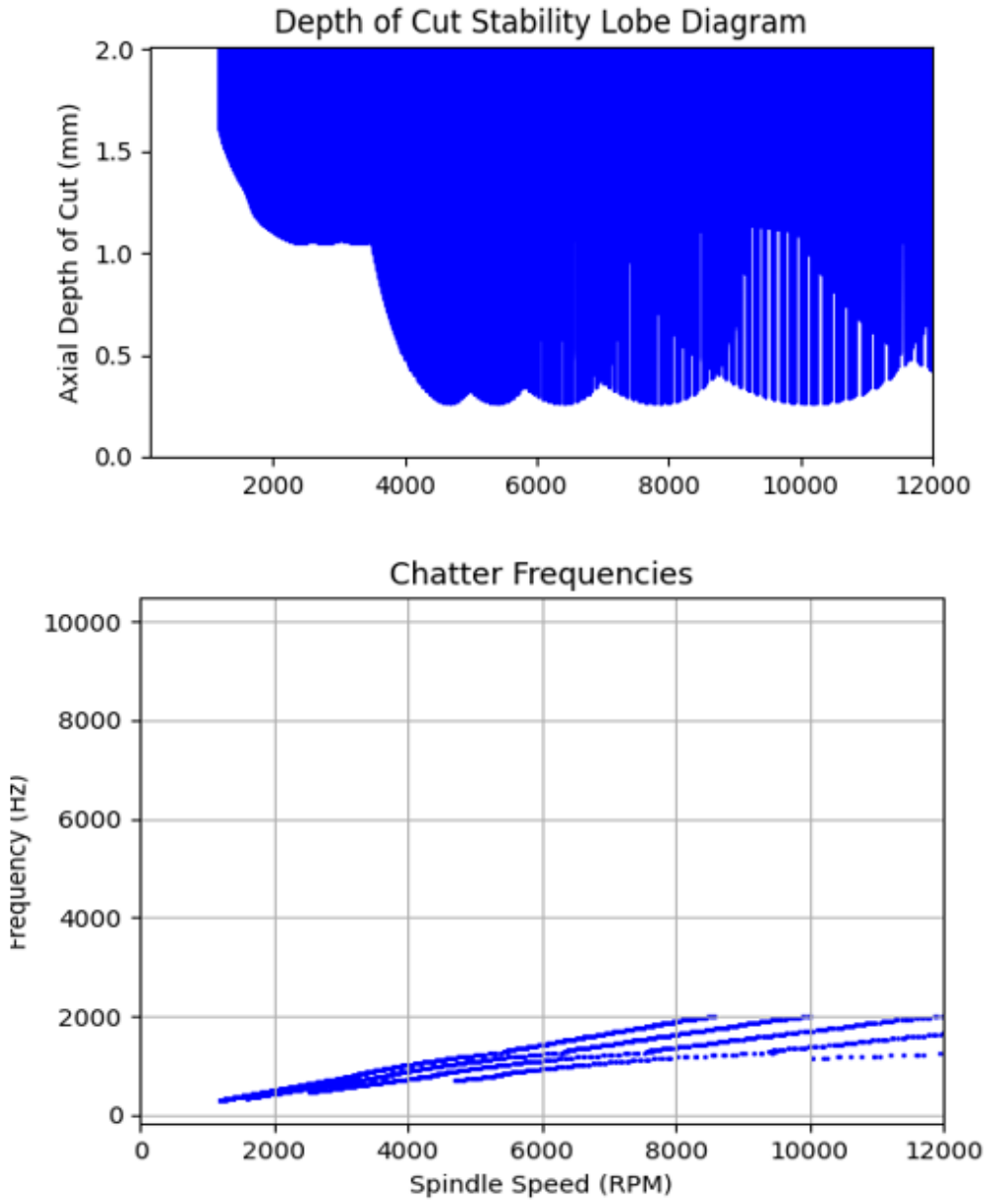

Figure 42 – Resulting SLD and chatter frequencies using the adapter.

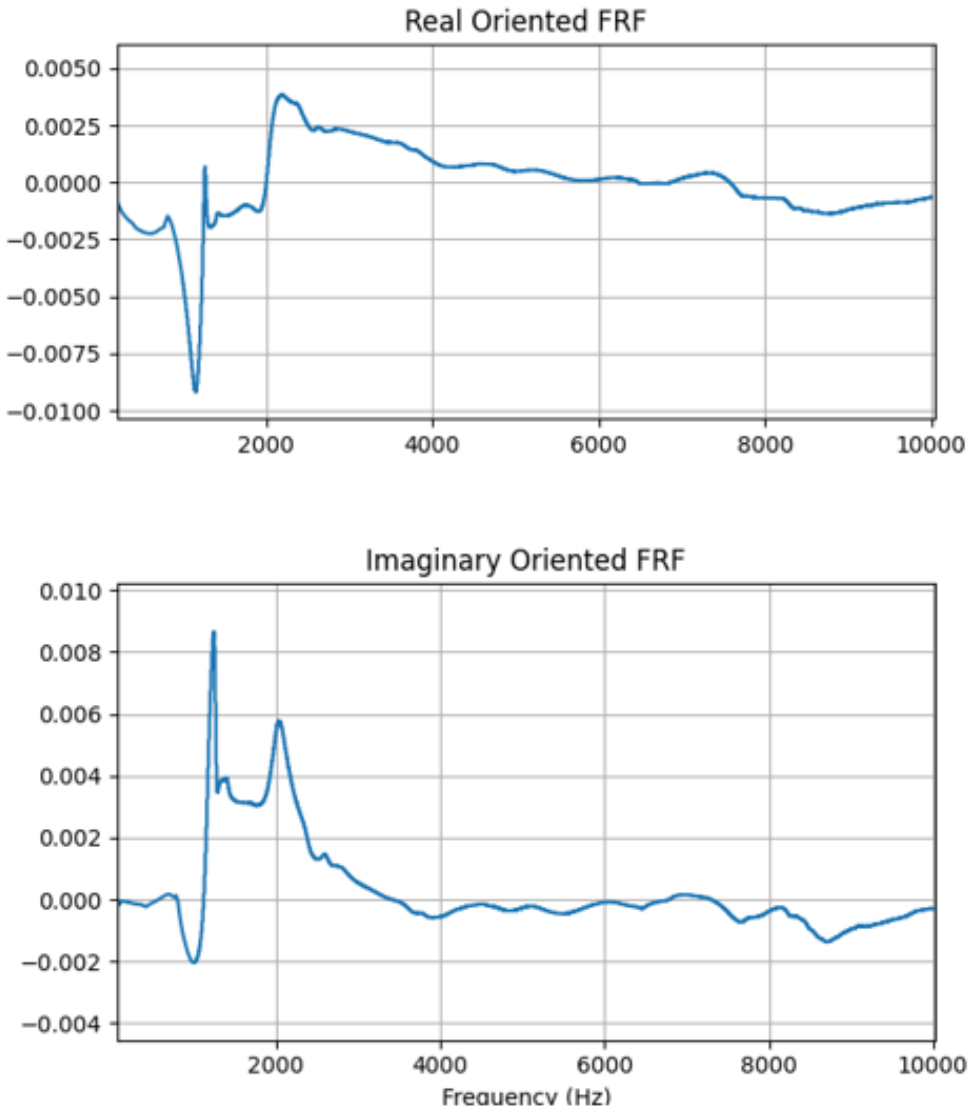

Figure 43 – Extracted FRF using SpinScope module.

More accurate and reliable results can be achieved by improving the taptest method, focusing on increasing the coherence. This method provides us FRFs that couldn´t be used on TFX, forcing us to generate an in-house code. Further development is needed to trust this method and introduce it into the industry.

10.4 Case Studies with External Companies

The technology was evaluated using two companies where different drilling tools were evaluated. The results show good results in an optimization process. The tests were carried out in a different project where the goal was focused on reducing energy consumption. Through the course of this project, we had the opportunity to test drill bits, find their modal frequencies, and the associated stability lobe diagrams for the operations.

10.4.1 Prodan A/S

Prodan is a state-of-the-art machine factory for metalworking and plastic processing, located in a 15,000 m² factory building with full crane capacity. Prodan machine shop is equipped for both complex and simple tasks within metalworking and plastic processing, including chipping, welding, sheet metal processing and heavy material processing.

The production item was a low-carbon steel S355J2 - 40 [mm] thick “U-shaped” plate. As we can appreciate (Figure 44), the machined part presents six holes where we focused our efforts. In this process, the holes are pre-made by drilling and finished using a milling process. This last consideration is important since the final surface analysis was not possible.

Figure 44 – Final machined part (left) and rough material (right).

The tool is modular consisting of a GTP insert (Table 2) mounted on a KenTIP™ FS with through coolant (Table 3).

Material Number	7002460
ISO Catalog ID	KTFST22000GTPM
Grade	KC7325
[D1] Drill Diameter	22 mm
[L5] Drill Point Length	3.62 mm
[SSC] Insert Seat Size	ZA

Table 2 - GTP insert specifications.

Material Number	6389335
ISO Catalog ID	KTFS0867R03SCF100
[D1] Drill Diameter M	22 mm
[D1MAX] Drill Diameter Maximum	22.999 mm
[L4] Maximum Drilling Depth	69 mm
[L] Overall Length	155 mm
[LATTH] Insert Attach LG Holder	86.2 mm
[L1] Insert Gage Length	99 mm
[LS] Shank Length	56 mm
[D] Adapter / Shank / Bore Diameter	25.4 mm
[SSC] Insert Seat Size	ZA

Table 3 – KenTIP tool body specifications.

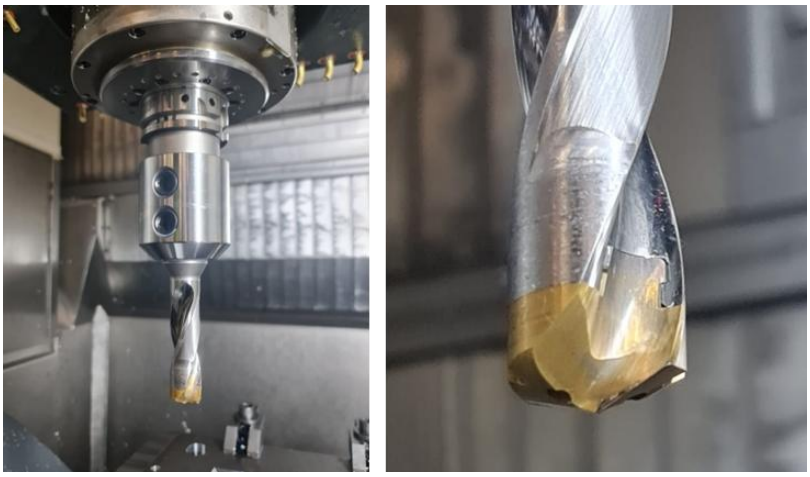

Figure 45 – 22 [mm] diameter modular drill bit.

The machine used for these tests was a 5-Axis DMC 85 monoBLOCK.

Figure 46 - CNC Machine used for Prodan drilling tests.

The company runs the tool using a cutting speed of 100 [m/min] and a feed per revolution of 0,25 [mm/rev]. As an initial assessment, we considered the feed per revolution well selected, and the cutting speed low (could be set up to 175 [m/min]).

After tap testing the tool using the boring module, we obtain the stability lobe diagram (Figure 47). We can see the selected parameters (blue dot) for this tool are inside the stable zone envelope (considering error margins).

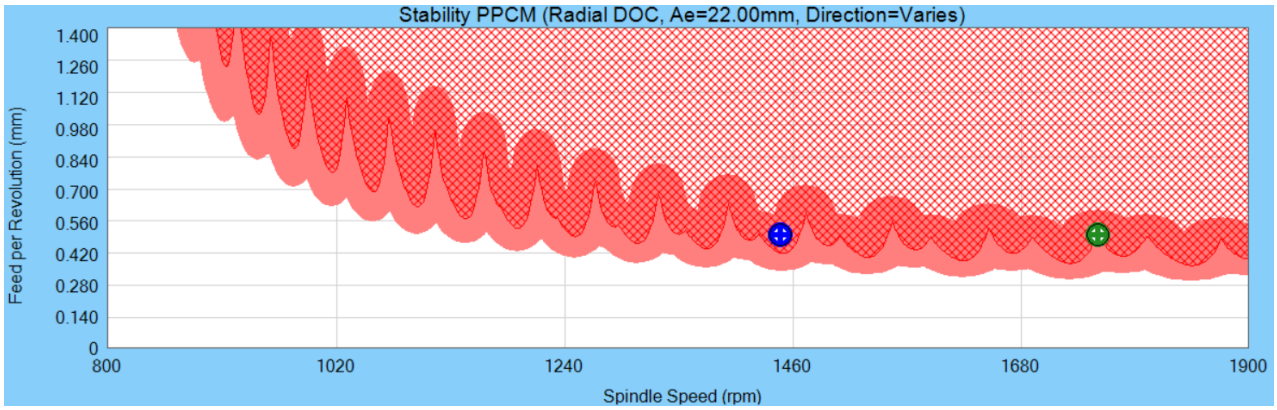

Figure 47 – Resulting Stability Lobe Diagram for a drilling process using 22 [mm] drill bit.

It is possible to select a better set of parameters just by synchronizing the spindle speed with a lobe (green dot) (Figure 47). In this case, procuring is not to exceed the maximum cutting speed. The optimized parameters are a cutting speed of 121[m/min], and the feed per revolution was not modified. DAMRC considered this change as a conservative approach that would not affect tool life considerably.

The resulting process with optimized parameters had an increase of 21% in material removal rate and a 17% in time reduction. The operator and DAMRC engineer, present on the test, did not feel any increase in noise level suggesting the tool remains in a stable condition.

10.4.2 KP Komponenter A/S

The company specializes in fully automated machining of complex parts, that supplies components directly to customer assembly lines. The company serves industries such as hydraulics, wind turbines, and offshore with advanced CNC machining, traditional manufacturing, and specialized processes. KP's expertise extends to small-series and large-scale production, supported by a strong network for surface treatment, hardening, and more. Renowned for turnkey solutions, KP combines product development, prototyping, and series production with strict adherence to tolerances.

In this case, the part material was medium-carbon steel. The part presents several standard holes which are finished using special drills (Figure 48). The analysed operation is a pre-drill of 13 [mm] diameter.

Figure 48 – Machined parts, optimized parameters (left) and base case part (right).

The tool is a 13[mm] drill bit with through coolant. The full tool description can be found in Table 4.

DC	Cutting diameter	13.000 mm
DMM	Shank diameter	14.00 mm
Gradetype	Gradetype	Carbide PVD
ItemNumber	Item Number	02899104
LCF	Length chip flute	60.0 mm
LFS	Functional length secondary	62.0 mm
LS	Shank length	45.0 mm
LU	Usable length	43.0 mm
OAL	Overall length	107.0 mm
PL	Point length	2.4 mm
SIG	Point angle	140.0 deg
Shanktype	Shanktype	Cylindrical
Weight	Net weight	0.170 kg
ZEFP	Peripheral effective cutting edge count	2

Table 4 – 13 [mm] diameter drill bit specifications.

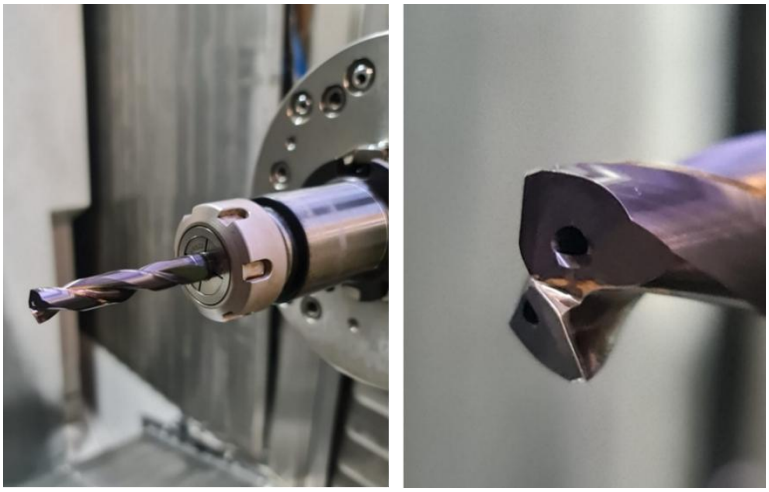

Figure 49 – 13 [mm] diameter integral drill bit.

The machine used for these tests was a 4-Axis Mazak HCN-5000.

Figure 50 – Machine used for KP Komponenter drilling tests.

The company runs the tool using a cutting speed of 100 [m/min] and a feed per revolution of 0,2 [mm/rev]. As an initial assessment, we considered the feed per revolution well selected, and the cutting speed low (could be set up to 130 [m/min]).

After tap testing the tool using the boring module, we obtain the stability lobe diagram (Figure 51). We can see the selected parameters (blue dot) for this tool are inside the stable zone envelope (considering error margins).

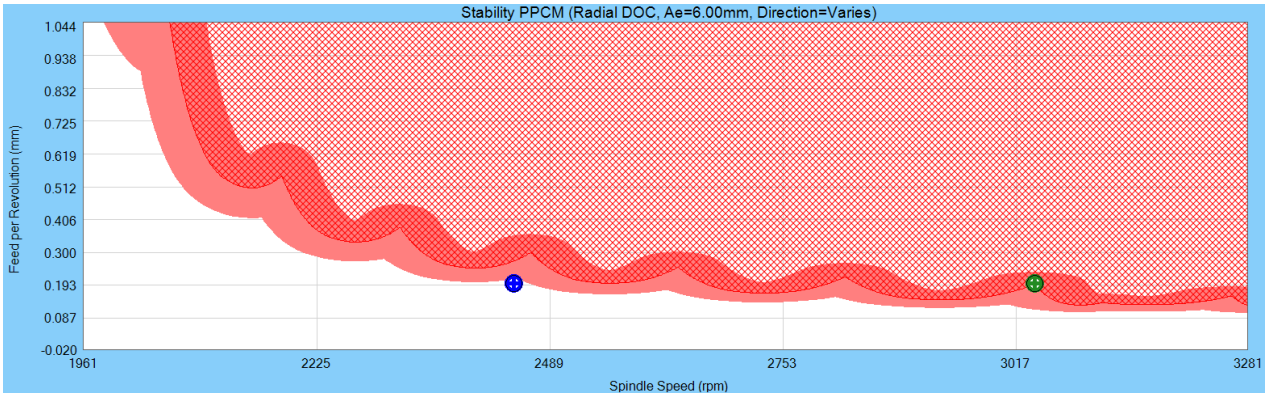

Figure 51 – Resulting Stability Lobe Diagram for a drilling process using a 13 [mm] drill bit

By synchronizing the spindle speed with a lobe (green dot) we can improve productivity parameters (Figure 51). In this case, procuring is not to exceed the maximum cutting speed. The optimized parameters are a cutting speed of 124[m/min], and the feed per revolution was not modified. DAMRC considered this change as a conservative approach that would not affect tool life considerably.

The resulting process with optimized parameters had an increase of 24% in material removal rate and a 19% in time reduction. The operator and DAMRC engineer, present on the test, did not feel any increase in noise level suggesting the tool remains in a stable condition.

It was found that the input tool parameters would have a considerable impact on the SLD. Thus, is important to set up the tool geometry correctly. Being able to translate boring parameters to other similar operations is especially important in drill bits.

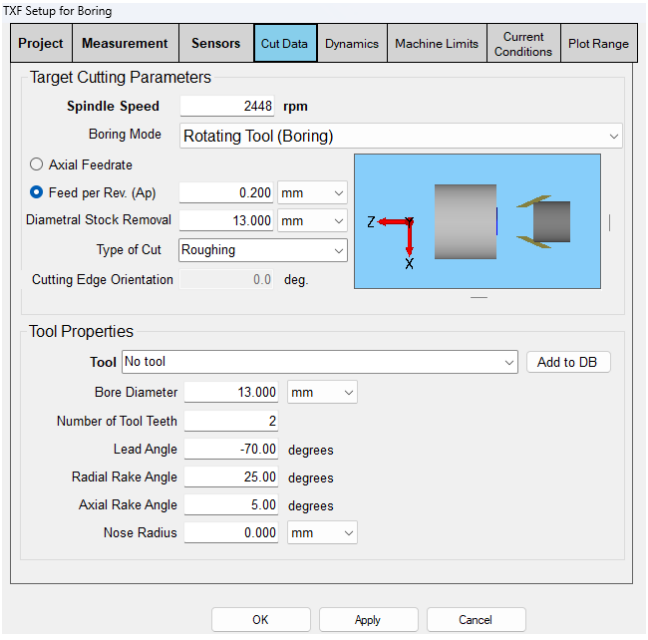

Figure 52 – Translated cut data parameters for drilling operation.

NOTE: Inside the setup tab for Boring process is important to translate the Bore Diameter (Boring) as the Tool Diameter (Drill bit), the Lead Angle (Boring) as half of the Point Angle (Drill bit), and the Radial Rake Angle (Boring) as the Helix Angle (Drill bit). By setting this parameter correctly we have achieved promising results.

In the Figure 52 is possible to see the parameters for a diameter 13 [mm] drill bit with a Point Angle of 140 [degrees], and a helix angle of 25 [degrees].

10.5 Partial Conclusion

A pre-analysis of the relevant features of TXF and a study of the relevant scientific literature were performed to inform in-house tests of the boring and helical milling modules in the software. Initial investigations demonstrated that the helical milling module is unable to generate SLDs due to a potential software bug and is unsuitable for either internal or external testing. The boring module, however, was found to have no such problems. The SLD obtained with the boring cutting module was found to be acceptable and was verified with cutting tests. The results obtained from internal testing of the boring module are supported by external test results obtained at case companies.

11 Discussion

Minor alterations were made to the activities outlined in the project application. Tap tests were performed on the DMU 80 CNC center according to the prescribed work packages in the application, however, these tests were extended to include cutting trials to validate the resulting SLDs. These cutting tests occurred only for the boring cutting module as discussed in sections 10. The suggested timeline in which the activities of the project were completed was also adjusted to accommodate the relocation of DAMRC in February 2024. The schedule pertaining to this relocation as well as the necessity of allocating the tap test equipment to multiple projects resulted in a delay in the planned activities of the project. Nevertheless, it is expected that all of the prescribed work will be completed on schedule within the allotted number of hours assigned to the project.

12 Conclusion

An upgraded version of the TXF software used for tap testing was acquired by DAMRC in 2022. The new software has additional software options to enhance process optimization, including additional cutting modules tailored to tap testing and optimizing more machining processes. The activities in this project focused on acquiring insights and competency in the use of two of these new modules that are of particular interest to the Danish industry. These two modules are Helical Milling and Boring. Helical Milling is a machining strategy used in pocket milling in which the cutting tool follows an orbital tool path as it plunges into the work material, while boring is a commonly used operation to enlarge pre-existing holes.

Initial investigations into the software identified several differences in the settings pertaining to configuring the measurement of tool and workpiece FRFs and cutting parameters. Subsequently, it was determined that the Helical Milling software does not produce actionable SLDs due to glitches in the software, while the Boring module had no such issues. It is worth mentioning that DAMRC has experience using the basic milling module for helical milling optimization processes with good results. The results obtained with the boring modules were then verified by cutting tests conducted in the DMU 80T machining centre at DAMRC.

From the activities of the project, confirmation was obtained that the boring cutting module is suitable for use in the industry for drilling operations in milling machines. Standard testing procedures and report formats were established for this purpose. This assessment was further supported by results obtained at case companies, which indicated optimizations in MRR and time reductions of approximately 20% and 15% respectively. The project can therefore be considered a success according to the criteria stated in the section 5 were achieved. Utilizing the boring module of TXF in relevant process optimization kickstarts or other projects is therefore highly recommended.

Appendix

Appendix A: Supplemental Results and Data for Boring Module Tap Tests

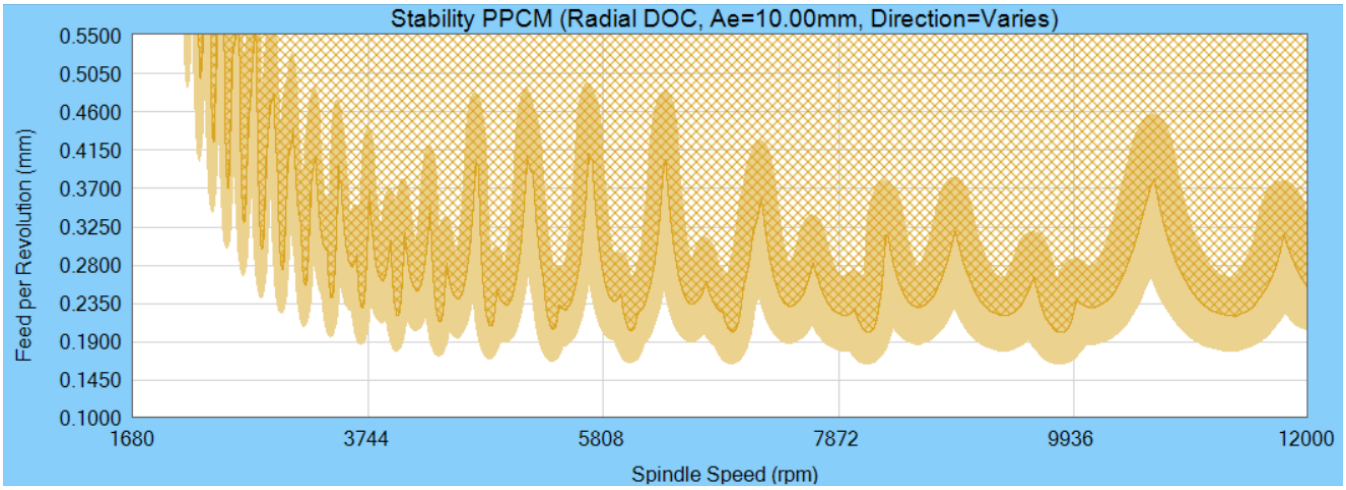

Figure A1 – Second detailed view of Figure 34, showing SLD for small (brown) hammer.

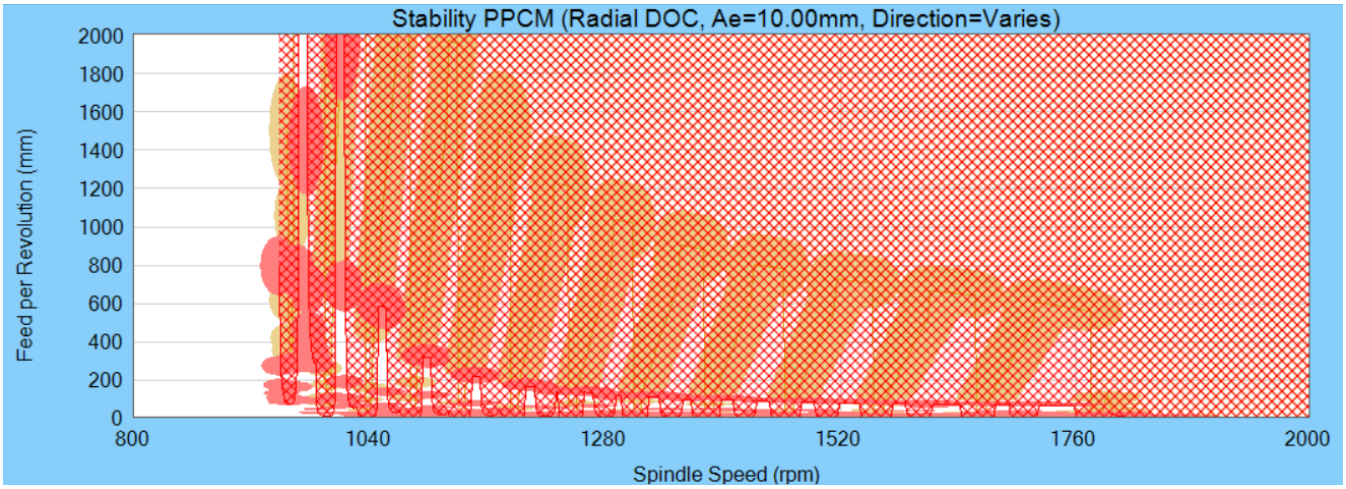

Figure A2 – Third detailed view of Figure 34, showing SLD for medium (red) and small (orange) hammer.

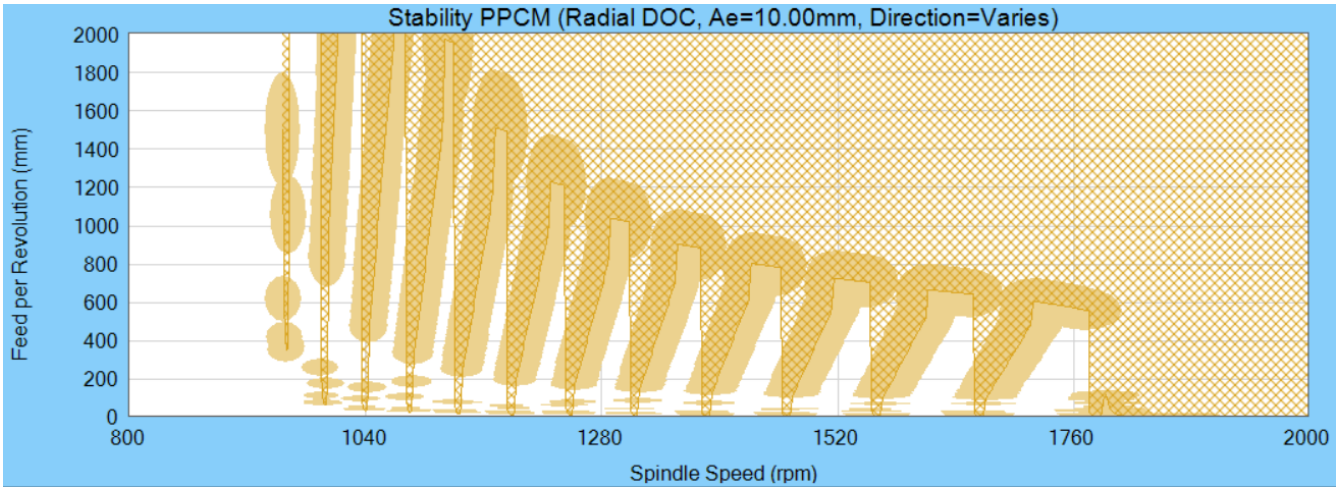

Figure A3 – Fourth detailed view of Figure 34, showing SLD for small (orange) hammer.

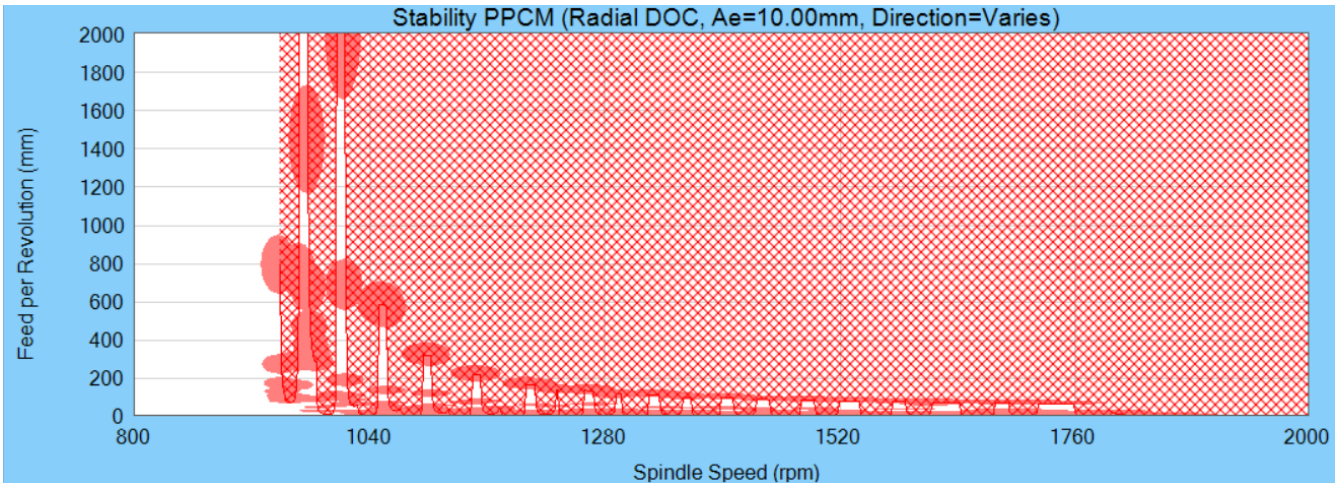

Figure A4 – Fifth detailed view of Figure 34, showing SLD for medium (red) hammer.

References

Altintas, Y. (2003). Mechanics of boring process - Part I. *International Journal of Machine Tools and Manufacture, 43*, 463-476.

Altintas, Y. (2003). Mechanics of boring processes - part II. *International Journal of Machine Tools and Manufature, 43*, 477-484.

Altintas, Y. (2006). Chatter Stability of Plunge Milling. *CIRP Annals, 55*(1), 361-364.

Altintas, Y. (2012). *Manufacturing Automation: Metal Cutting Mechanics, Machine Tool Vibrations, and CNC Design* (2nd ed.). Vancouver: Cambridge University Press.

Budak, E. (2007). Analytical Modeling of Chatter Stability in Turning and Boring Operations - Part I: Model Development. *Journal of Manufacturing Science and Engineering, 129*(4), 726-732.

Dong, Y. (2014). Cutting force prediction and analytical solution of regenerative chatter stability for helical milling operation. *International Journal of Advanced Manufacturing Technology, 73*, 433-442.

Schmitz, T. (2020). Uncertainty evaluation for twist drilling stability model. *Precision Engineering, 66*, 324-332.

Zhang, W.-H. (2019). Dynamics of tapping process. *International Journal of Machine Tools and Manufature, 140*, 34-47.